MTL TR 91-17

AD

FATIGUE RESISTANT OPTICAL FIBERS

GEORGE G. BRYANT
CERAMICS RESEARCH BRANCH

May 1991

Approved for public release; distribution unlimited.

US ARMY
LABORATORY COMMAND
MATERIALS TECHNOLOGY LABORATORY

U.S. ARMY MATERIALS TECHNOLOGY LABORATORY
Watertown, Massachusetts 02172-0001

UNCLASSIFIED

SECURITY CLASSIFICATION OF THIS PAGE *(When Data Entered)*

REPORT DOCUMENTATION PAGE		READ INSTRUCTIONS BEFORE COMPLETING FORM
1. REPORT NUMBER MTL TR 91-17	2. GOVT ACCESSION NO.	3. RECIPIENT'S CATALOG NUMBER
4. TITLE *(and Subtitle)* FATIGUE RESISTANT OPTICAL FIBERS		5. TYPE OF REPORT & PERIOD COVERED Final Report 6. PERFORMING ORG. REPORT NUMBER
7. AUTHOR*(s)* George G. Bryant		8. CONTRACT OR GRANT NUMBER*(s)*
9. PERFORMING ORGANIZATION NAME AND ADDRESS U.S. Army Materials Technology Laboratory Watertown, Massachusetts 02172-0001 SLCMT-EMC		10. PROGRAM ELEMENT, PROJECT, TASK AREA & WORK UNIT NUMBERS D/A Project: ID464810DC26
11. CONTROLLING OFFICE NAME AND ADDRESS U.S. Army Laboratory Command 2800 Powder Mill Road Adelphi, Maryland 20783-1145		12. REPORT DATE May 1991 13. NUMBER OF PAGES 33
14. MONITORING AGENCY NAME & ADDRESS *(if different from Controlling Office)*		15. SECURITY CLASS. *(of this report)* Unclassified 15a. DECLASSIFICATION/DOWNGRADING SCHEDULE

16. DISTRIBUTION STATEMENT *(of this Report)*

Approved for public release; distribution unlimited.

17. DISTRIBUTION STATEMENT *(of the abstract entered in Block 20, if different from Report)*

18. SUPPLEMENTARY NOTES

19. KEY WORDS *(Continue on reverse side if necessary and identify by block number)*

Fiber optics	Fracture mechanics
Dynamic tests	Protective coatings
Fatigue tests	Stress corosion

20. ABSTRACT *(Continue on reverse side if necessary and identify by block number)*

(SEE REVERSE SIDE)

DD FORM 1 JAN 73 1473 EDITION OF 1 NOV 65 IS OBSOLETE

UNCLASSIFIED

SECURITY CLASSIFICATION OF THIS PAGE *(When Data Entered)*

Block No. 20

ABSTRACT

Certain requirements in commercial and military communications and guidance systems have prompted the development of high-strength, fatigue-resistant optical fibers for uncabled applications. The most significant environmental factors degrading the strength of glass fibers over time are stress and hydroxyl ion attack on glass surfaces. Several solutions have been formulated and attempted; these include increased bulk-strength glass and hermetic or passivating coatings. Test and evaluation of several commercially available fibers incorporating these promising solutions have been made using various fatigue and aging scenarios. Static-fatigue prediction from analysis of various constant extension rates to failure, termed in the literature and here as dynamic-fatigue, was also investigated.

CONTENTS

	Page
INTRODUCTION	1
EXPERIMENTAL	3
RESULTS	5
DISCUSSION	9
SUMMARY	15
ACKNOWLEDGMENTS	15
APPENDIX A	16

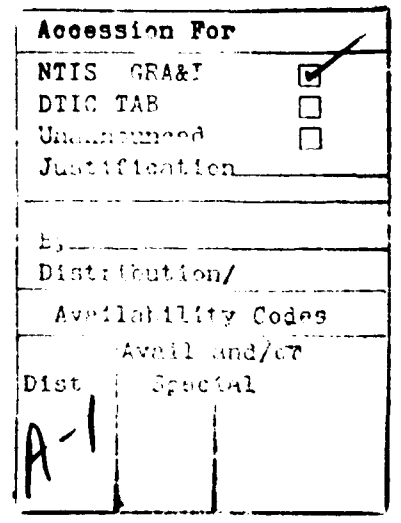

INTRODUCTION

The most significant drawback to the design, production, and utilization of optical fibers is the lack of long-term mechanical reliability. This is most important in uncabled configurations such as in Fiber Optic Guided Vehicle (FOG-V) payout systems, where the glass core and cladding must provide the structural, as well as the signal transmission, function of the link component. Polymer-coated optical glass fibers subjected to static fatigue demonstrate a deterioration in resistance with time. Plotted data of log stress versus log time to failure produce curves with slopes negative N (fatigue-resistance constant) which have values of 15 to 20 for the high-stress, short-time regime and deteriorate to values of 1 to 8 in the low-stress, long-time regime. Increasing test temperature accentuates this deterioration. This non linear behavior makes static-fatigue lifetime predictions at very long-time, low-stress inaccurate; therefore, long-term performance is difficult to guarantee.

In light of these problems, industry has sought solutions to deteriorating strength through process optimization which increases initial bulk strength through flaw suppression. Increased strength retention through numerous coating scenarios has also been attempted. Hermetic and passivating coatings inhibit introduction of glass surface active species such as hydroxyl ions, which generate flaws, and slow the growth of intrinsic surface flaws. Hermetic coatings are generally of the metallic or ceramic variety; they are typically applied by vapor deposition prior to standard polymeric buffer coatings. Passivating coatings are specialized polymeric materials which are usually applied instead of standard polymer buffers. Hermetic coatings have the disadvantage of applying a residual stress at the glass cladding/hermetic coating interface that may diminish the initial inert strength of the fiber. The goal of hermetic/passivating barriers is to prevent the fatigue transition, observed N deterioration discussed above, which can dramatically affect mechanical strength and make system performance highly speculative.

This fatigue transition has been attributed to the combination of zero-stress aging with static fatigue. France et al.[1] developed a model for this effect which assumes that for the first half of the lifetime zero-stress aging controls strength degradation; static fatigue controls it for the second half. Static-fatigue behavior can be characterized by the time to failure, t_f, as a function of applied stress, S_a, in the following equation:[2]

$$t_f = B S_i^{(N-2)} / S_a^{N} \qquad (1)$$

where B is a material parameter, N is the fatigue resistance constant described above, and S_i is inert strength. These factors are the same ones exploited in the power law approximation of crack-growth-controlled dynamic fatigue:[3-5]

$$S_f^{(N+1)} = B(N+1)\dot{S} S_i^{(N-2)} \qquad (2)$$

1. France, P. W., et al. *Strength and Fatigue of Multicomponent Optical Glass Fibers.* Journal of Materials Science, v. 18, no. 3, 1983, p. 785-792.
2. Kalish, D., and Tariyal, B. K. *Static and Dynamic Fatigue of a Polymer-Coated Fused Silica Optical Fiber.* Applied Physics Letters, v. 28, 1976, p. 518-523.
3. Ritter, J. E., Service, T. H., and Guillemet, C. *Strength and Fatigue Parameters for Soda-Lime Glass.* Glass Technology, v. 26, no. 6, 1985, p. 273-278.
4. Ritter, J. E., Glaesemann, G. S., Jakus, K., and Rampone, P. *Dynamic Fatigue of Soda-Lime Glass as a Function of Temperature.* Physics and Chemistry of Glasses, v. 27 no. 2, 1986, p. 65-70.
5. Ritter, J. E., Jakus, K., and Service, T. H. *Measurement of the Fatigue Behavior of Optical Glass Fibers.* Final report under Contract No. DAAG29-81-D-0100, Delivery Order 2509, Scientific Services Program, U.S. Army Materials Technology Laboratory, Watertown, MA.

where S_f is failure stress and $\dot{S}$ is stressing rate.

France also established an empirical relationship for zero-stress aging behavior:

$$S_i = S_{io}(1+at)^b \tag{3}$$

where S_i is inert strength at time t, S_{io} is inert strength at t = 0, and a and b are scaling constants which come from linear log (1+at) versus log (S_i) plotted data. Assuming that zero-stress/static-fatigue combined behavior follows the France scenario, allowing t_f to equal $t_f/2$ in both Equation 1 and Equation 3 and combining them gives the following modified static fatigue equation,

$$t_f = 2B[S_{io}(1+at_f/2)^b]^{(N-2)}/S_a{}^N. \tag{4}$$

From theory, B is a material parameter derived from the power law expression for crack velocity, $V = c \exp(-E/RT) * (K_I/K_c)^N$,[3,4] or empirically $V = AK_I N$.[1] This power law expression produces the Equation 2 for dynamic fatigue behavior, where

$$B = 2K_{Ic}{}^2/[(N-2)AY^2] \tag{5}$$

and

$$A = c\exp(-E/RT). \tag{6}$$

Here, K_{Ic} is the critical stress intensity factor (approximated here as 0.79 MPa-$m^{1/2}$ for fused silica), Y represents the crack loading and flaw geometry (approximately 1.24),[2] R the ideal gas constant (8.314 j/mol-°K), T absolute temperature in °K, c a pre-exponential constant, and E the empirical measurement of zero-stress activation energy.

Given data from dynamic fatigue experiments (constant strain rate to failure) on unaged fiber at several stressing rate levels, plots of ln(S) versus ln(S_f) yield the slope 1/(N+1). Repeating experiments at a different temperature results in a second line which used in linear regression will yield E and B′:

$$B' = 2K_{Ic}{}^2/[(N-2)cY^2] \tag{7}$$

where B′ is the component of B that will appear nearly constant with temperature in regions where N is independent of temperature (short time to failure). Components of B′ are not discussed in more detail here, as the subtleties of the various contributions are assumed to not contribute significant variation in B between usage in the static and dynamic behaviors represented by Equation 1 and Equation 2. More appropriate values of K_{Ic} and Y may be obtained from fractographic analysis of origin of failure flaws and other geometrical aspects of the sample and test, but are not specifically required for this analysis and are beyond the scope of this report.

Given data from dynamic fatigue experiments on zero-stress aged fiber, the scaling constants for Equation 3 can be estimated by achieving a "best fit" line on a $\ln(1+at)$ versus $\ln(S_f)$ plot through guessing at values for a. The resultant a and b values can then be used with the other material constants determined for Equation 2 to estimate t_f with Equation 3 for modified static fatigue. Data which produce lines that have zero slope or slightly positive slopes for all values of a do not exhibit zero-stressed aging deterioration. The pure static fatigue Equation 1 is then the appropriate estimator for t_f.

Similar mechanical testing and analysis done by Ritter, et al.[5] was sponsored by the U.S. Army Materials Technology Laboratory (MTL) in 1986 as part of an effort to promote low-cost, high-strength optical fibers for FOG-M and similar systems. The fibers tested were in multi-mode format as opposed to the single-mode fibers tested here, and were early 1986 "vintage" developments. The fibers tested in this study were late 1988 "vintage" developments, and were assumed to reflect the general quality improvements underway in the optical fiber industry during this timeframe. Two of the contributing manufacturers were the same between these two studies, Corning and Ensign Bickford. The predicted static fatigue behaviors for these fibers were marginally different between 1986 multi-mode and 1988 single-mode versions.

EXPERIMENTAL

Five optical fibers used in this study were obtained directly from manufacturers. The study focused on single-mode, 125 micron diameter clad fiber taken from stock considered to be "resistant" to fatigue for use in uncabled systems. Several of the manufacturers who provided fiber for the studies by Ritter, et al.[5] also provided fibers for the work at MTL, from more recent developmental "generations," and in single-mode format. All manufacturers except GTE have commercially available military-grade fiber on the market. One of the fibers provided was not included in the full series as it did not comply with several of the requested specifications. American Telephone & Telegraph (AT&T) and Corning used "hermetic" coatings on their fibers, Ensign Bickford used a "hard coat" polymer (then in the experimental stage), and GTE used a developmental polymer. These coatings were to meet the challenge of preventing the static fatigue transition which occurs in conventional polymer-coated fiber. Fiber types will be indicated by number and the manufacturer will remain unspecified.

Fibers were aged in distilled water at 65°C in a regulated tank (+/- 0.5°C) for various lengths of time. Three "stressing" conditions were tried for aging: unstressed (6 cm minimum bend radius), bending stressed (0.31 cm radius mandrel under 100 grams to 125 grams winding tension), and tensile stressed (430 grams tension between 2.5 cm radius shafts) which correspond to 10 KPSI/69 MPa, 215 KPSI/1450 MPa, and 50 KPSI/340 MPa stress, respectively. These approximated stresses are calculated knowing applied loads, bend deformations, fiber geometry, and Young's modulus for the glass component of the optical fiber. Here, as elsewhere in the analysis, the hermetic coatings and polymer buffers are not considered to contribute significantly to the optical fiber's load bearing and stress/strain characteristics. This is due to either minimal relative cross-sectional area or much lower Young's modulus than that of the glass.

Dynamic fatigue breaks, constant crosshead velocity to failure, were carried out on a universal testing machine. A gauge length of 0.1 meter was held between two 0.1 meter diameter fixed wheels coated with plastic tape and gripped by 0.05 meter diameter cams, as shown in Figure 1. This arrangement distributes the gripping force over a large length of the fiber and greatly reduces incidence of fracture at the gripping points caused by concentrated surface loads. The gauge length was inserted through a serum bottle stopper into a glass con-

denser tube filled with distilled water. Water temperature was held constant (+/- 0.5°C) with condenser jacket waterfed by a heater/circulator. Breaks that occurred outside this water filled region were discarded from the data set. Three crosshead velocities (2, 0.2, and 0.02 in./min) were used that correspond to stressing rates of approximately 1, 10, and 100 MPa. All aging groups were tested at 25°C (wet), and unaged groups were also tested at 80°C (wet) and 25°C in dry (18% to 22% relative humidity) air. The dry air environment was for approximation of inert strength, and samples were desiccated prior to breaking.

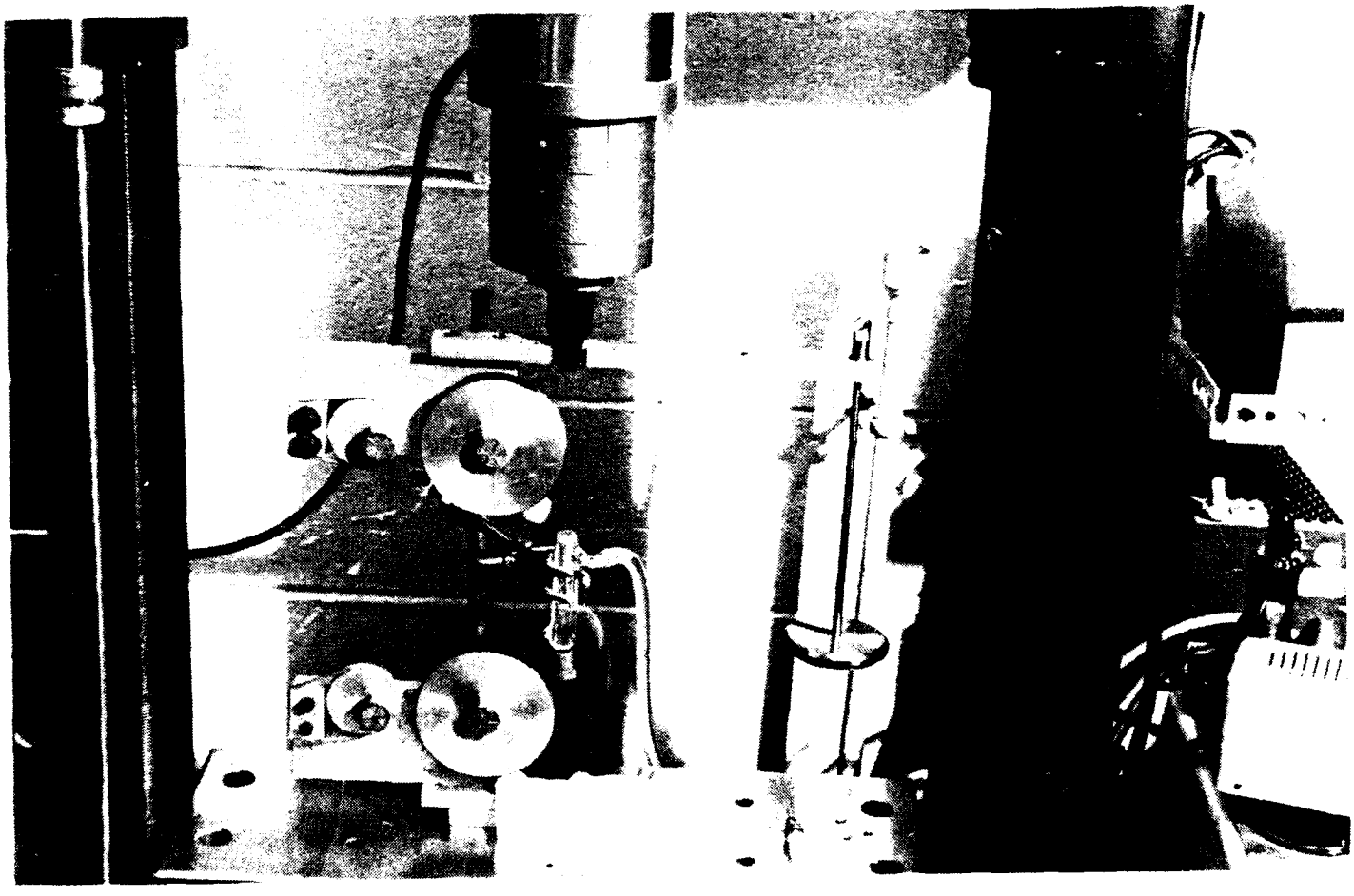

Figure 1. Dynamic fatigue test fibers.

Test data were recorded on a strip chart directly from load cell signals. Failure stress and stressing rate at failure were determined from the strip chart. Stressing rates were generally linear, except upon initial loading.

Each of the fibers was received on a spool with 1.0 to 2.2 kilometers of fiber wound loosely on it. From each spool several hundred 1.5 meter samples were cut and randomized prior to grouping for appropriate aging and dynamic fatigue tests. The aging and test matrix is described in Table 1.

Table 1. AGING AND TEST MATRIX

Break Condition & Media	°C	Aging Condition	Fibers Tested											
			# 1			# 2			# 3			# 4		
			Traverse Head Rate (in./min)											
			2.	0.2	0.02	2.	0.2	0.02	2.	0.2	0.02	2.	0.2	0.02
Air 18-22% R.H.	25	Unaged (desiccated)	X			X			X			X		
Water	80	Unaged	X	X	X	X	X	X	X	X	X	X	X	X
Water	25	Unaged	X	X	X	X	X	X	X	X	X	X	X	X
		[Aged 60°C in water] Zero-Stress (70 MPa)												
		20 hours	X	X	X	X	X	X	X	X	X	X	X	X
		100 hours	X	X	X	X	X	X	X	X	X	X	X	X
		500 hours	X	X	X	X	X	X	X	X	X	X	X	X
		2450 hours	X	X	X	X	X	X						
		Bend Stress (1450 MPa)												
		44 hours	X	X	X	X	X	X	X	X	X	X	X	X
		212 hours	X	X	X	X	X	X	*			X	X	X
		1052 hours	X	X	X	X	X	X	*			X	X	X
		Tensile Stress (340 MPa)												
		24 hours	X			X	X	X	X	X				
		190 hours		X			X			X		X	X	X

* Fiber 3 failed during extended aging.

RESULTS

The dynamic fatigue test strength data were fitted to a two parameter Weibull statistical distribution:[5]

$$\ln \ln [1 / (1-P_f)] = m \ln (S_f / S_o) \tag{8}$$

where P_f is the cumulative probability of failure, m and S_o are the slope and scale (intercept) parameters, and S_f is fracture strength. S_o is the stress value taken at the log plot intercept where P_f is actually 0.632, and is referred to as characteristic strength of the sample.

Throughout the following discussion P_f will always be relative to the sample size, not to unit volume. Tables A1a through A4a in Appendix A summarize the fatigue strength distributions of the four unaged fibers. Tables A1b through A4b in Appendix A summarize the fatigue strength distributions of the four fibers subsequent to aging in water for various times under several static stressing situations.

Tables A1 through A4 in Appendix A were very useful in establishing trends in the behavior of the fibers, such as relative sensitivity to moisture, temperature, stress rate, zero-stress aging, and low-stress aging. These trends are summarized in Table 2.

Table 2. DYNAMIC FATIGUE TRENDS
(RESULTANT % DECREASE IN S_o FROM CONDITION CHANGE)

Fiber	Wet Break	Hot Break	100-1 MPa/s	Age	Stress (aging)	P_f = 1%	Bimodal	m_{avg}
1	2 23@1%P_f	3-4	2-4	1-3 2450 hr	<2	2-25	Yes*	55(34)
2	13-15	8-18	15-20	9-15 2450 hr	<2	0-17	No	74(29)
3	12-14	8-22	18-27	19-26 500 hr	2-10	6-19	No	46(21)
4	9 32@1%P_f	13-18	17-23	<1 500 hr	<3	3-19	Yes†	62(37)

Values reported as +/- one standard deviation, or avg (std. dev.).

*Fiber 1 bimodal in 35% of plots.
†Fiber 4 bimodal in 15% of plots.

Table 2 displays percent decrease in failure strength attributed to the introduction of an imposed condition change. For example, decreasing the stress rate from 100 MPa/s to 1 MPa/s results in an observed 2% to 4% loss in strength for Fiber 1, the range coming from the several different aging condition sets. Similar trends can be observed for breaking in: water as opposed to air, hot water as opposed to cool water, aged fiber as opposed to unaged fiber, stress-aged fiber as opposed to unstressed-aged fiber, or by observing the strength distribution at P_f = 1% as opposed to 63.2%.

An important observation is that the (dry) air break strength S_o is significantly higher than that for wet breaks except for Fiber 1. This moisture sensitivity is more typical of conventional polymer-coated fibers. Fiber 1 does, however, exhibit a 23% difference at the P_f = 1% low-strength tail. This low-strength tail is the criterion by which uncabled fiber optic systems must be designed.

Figures 2 through 5 illustrate the strength distributions of the four fibers for unaged dynamic breaks under dry, wet, and hot and wet conditions. Figure 2 clearly illustrates the narrow strength distributions expected of high quality fibers, but the large disparity of inert strengths between fibers. In Figure 3 the bimodal behaviors of Fibers 1 and 4 are distinct, and somewhat typical of behavior found in aged breaking strength. Figure 4 shows the only example of distinct bimodal behavior in Fiber 2, for the 1 MPa/s hot broken condition. Bimodal behavior is typified by this flattening of the lower-strength tail, indicative of more than one strength controlling flaw population. This alternative flaw population appears to become activated by introduction of some adverse condition like elevated temperature or

aging. In this lone case of Fiber 2, it may be caused by surface damage due to handling and independent of the "controlled" test matrix parameters. Upper-strength tail flattening can, to a lesser degree, inuicate bimodal behavior as well. This can be seen in Figure 5 for both Fibers 3 and 4.

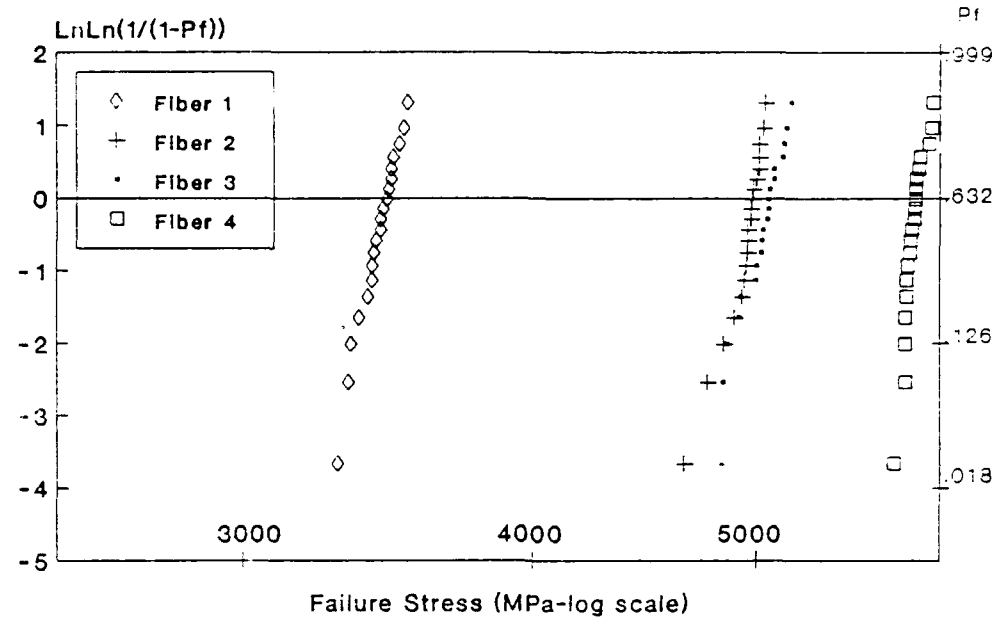

Figure 2. Dry breaking strength Weibull plots (100 MPa/s).

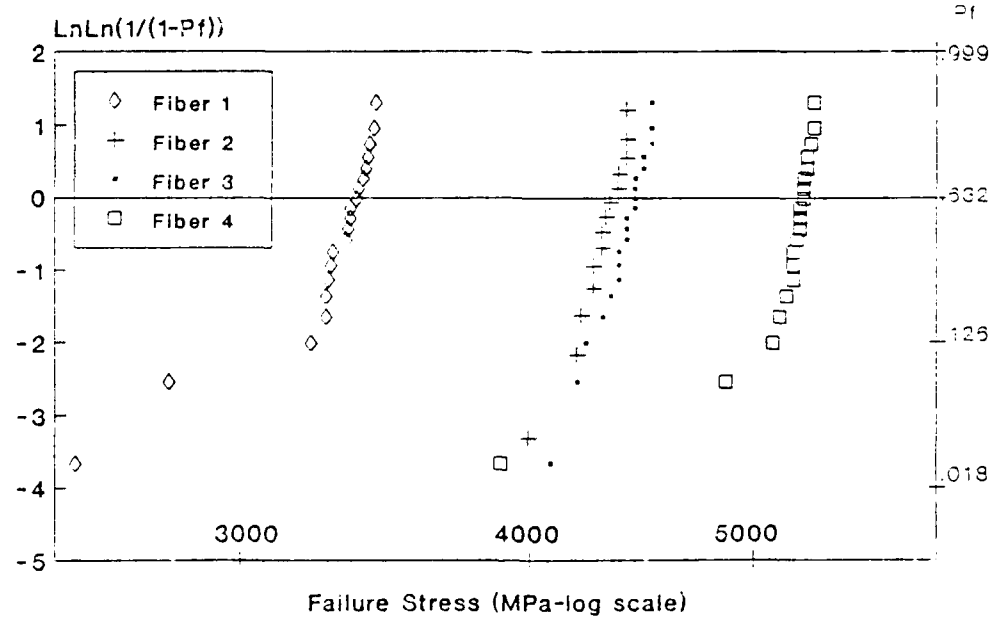

Figure 3. Wet breaking strength Weibull plots (100 MPa/s).

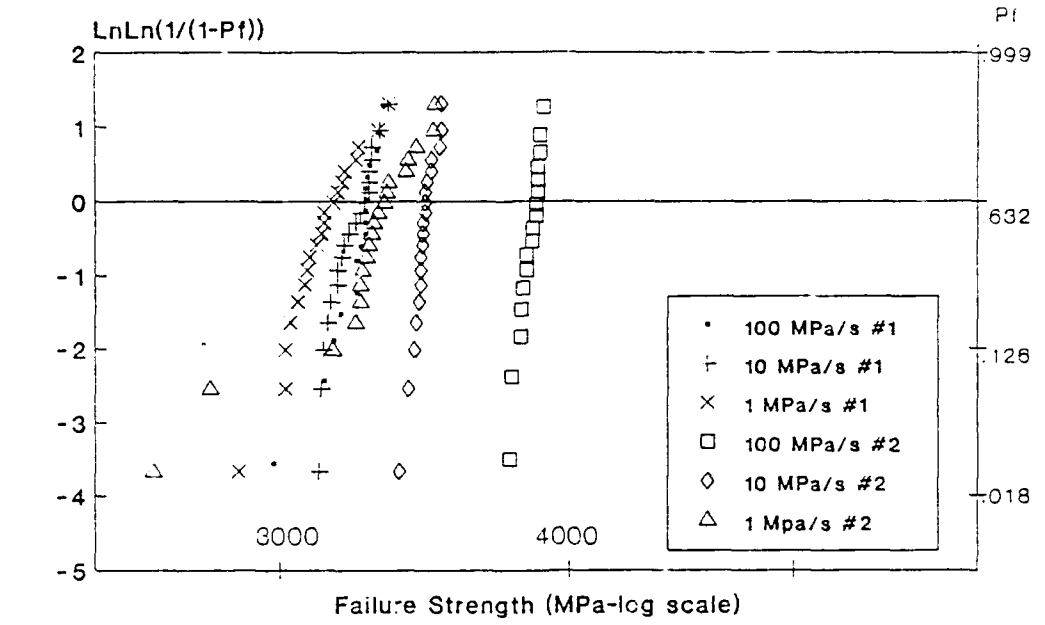

Figure 4. Wet-Hot breaking strength Weibull plots Fibers 1 and 2.

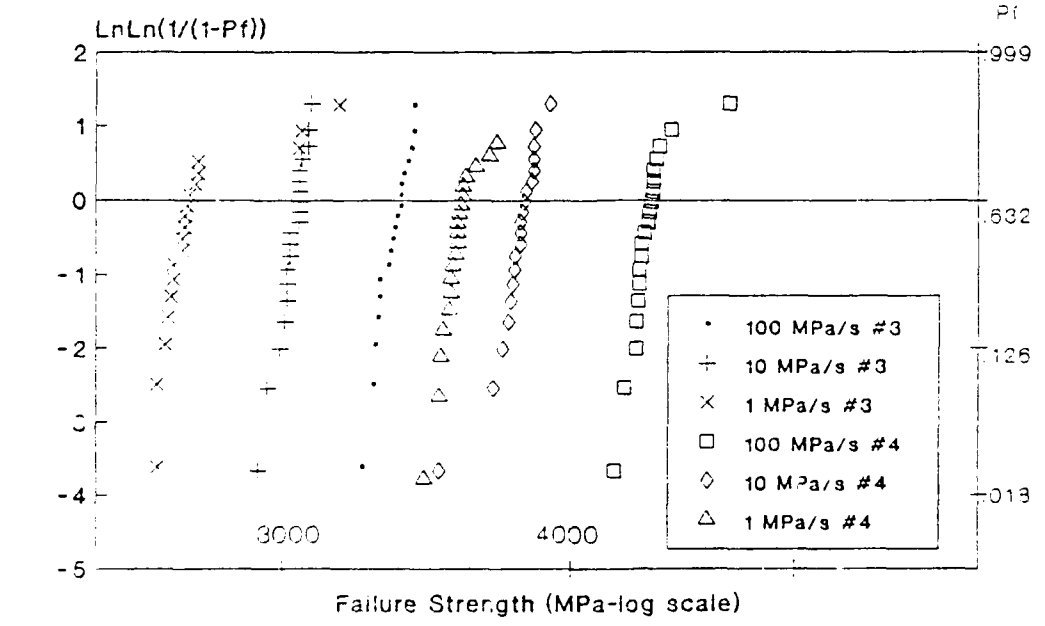

Figure 5. Wet-Hot breaking strength Weibull plots Fibers 3 and 4.

Figures A1 through A16, found in Appendix A, demonstrate the strength distributions for zero-stressed (see Figures A1 to A12) and low-stressed (see Figures A13 to A16) aged fibers. The broad and somewhat even spacing of the aging time lines across the strength axis for Fibers 2 and 3, (see Figures A2, A3, A6, A7, A10, and A11) indicate a large sensitivity to aging, which is especially noticeable due to the consistently well-behaved and narrow strength distributions. Fibers 1 and 4 (see Figures A1, A4, A5, A8, A9, and A12) have far less sensitivity to aging, but due to some bimodal behavior, this sensitivity is observed in the low-strength tails of Fiber 1. Comparison of plots between figures for stressing rate sensitivity shows similar significant strength gains for Fibers 2, 3, and 4 at the higher rates. This indicates sensitivity to dynamic fatigue. Low-stressed aging had little effect on dynamic fatigue strength in comparison to zero-stressed aging in general.

The appearance of the polymer coating did not change for Fibers 1 and 2, but 3 and 4 both showed some yellowing, particularly Fiber 3 for longer aging times and stressed conditions. It is important to point out that Fiber 3 exhibited numerous fracture failures on each of the six aging mandrels prior to 212 hours in the 1450 MPa bending stressed state and that the coating was extremely yellowed and somewhat opaque. The color changes are likely related to long-range chemical changes occurring in the coating or at the glass cladding/polymer coating interface or both.

DISCUSSION

The power law expression, as shown in Equation 2, can be put in natural logarithm form to enable determination of fatigue parameters.

$$(N+1)\ln(S_f) = \ln(\dot{S}) + \ln(N+1) + (N-2)\ln(S_i) + \ln(B') + [E/RT] \qquad (9)$$

From linear regression analysis of the dynamic fatigue data with $\ln\dot{S}$ and $1/T$ as the independent variables and $\ln(S_o)$ values for $\ln(S_f)$ as the dependent variable, the fatigue parameters N, E, and B′ are determined. The "space" between the two temperature lines of each fiber represents the temperature-sensitive component of $S_f \cdot [E/RT]/(N+1)$, E being the empirical activation energy. Figures 6a through 6d, Failure Stress versus Stress Rate, present these lines used in linear regression, and Table 3, Dynamic Fatigue Parameters, summarizes the results. The 90% confidence interval for the data points is shown in Figure 6, as well as the 90% confidence interval about the calculated lines, using common N value (N_c) from hot and cold averaged independent N's (Ni), at the endpoints. Fibers 3 and 4 have parameters very typical of conventional polymer-coated fiber with N about 20. Fibers 1 and 2 compare more closely in E and B′ parameters, but the extremely high N value for Fiber 1 indicates very stable characteristic strength, low stress rate sensitivity. It does not, however, take into account the low-strength tail bimodal behavior of Fiber 1, which would reduce the effective N value significantly. Due to the inconsistent nature of the bimodal behavior and the inaccuracies in a two-parameter Weibull distribution for sample size 20 at P_f = 1%, no additional analyses for fatigue parameters were performed at low-probability strength levels for either Fiber 1 or 4.

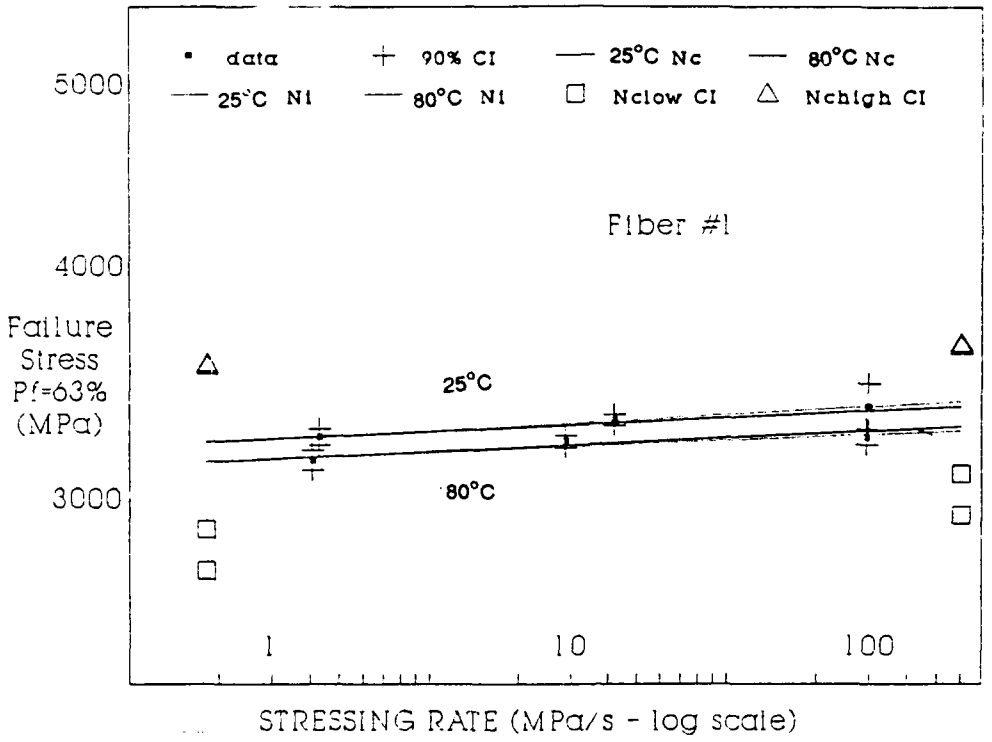

Figure 6a. Failure stress versus stress rate.

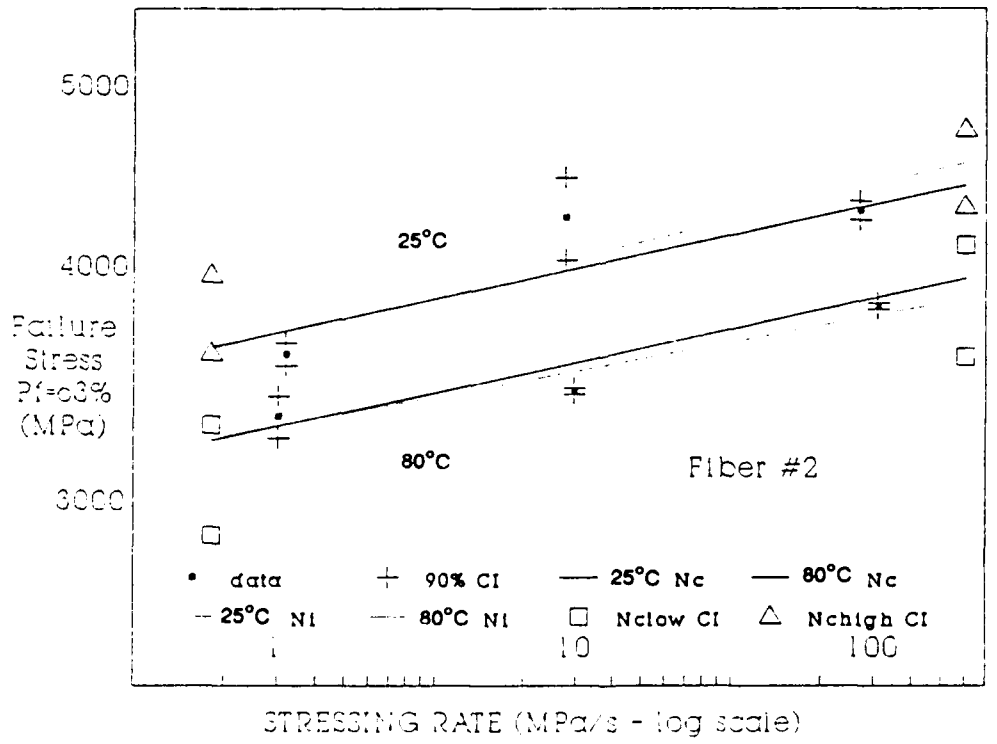

Figure 6b. Failure stress versus stress rate.

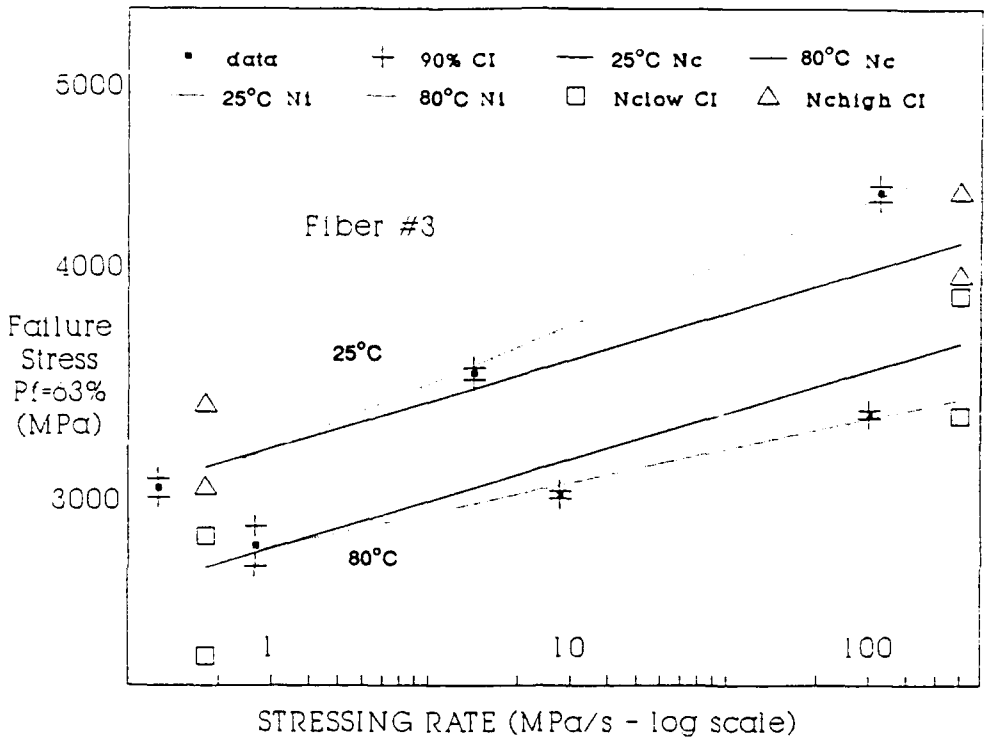

Figure 6c. Failure stress versus stress rate.

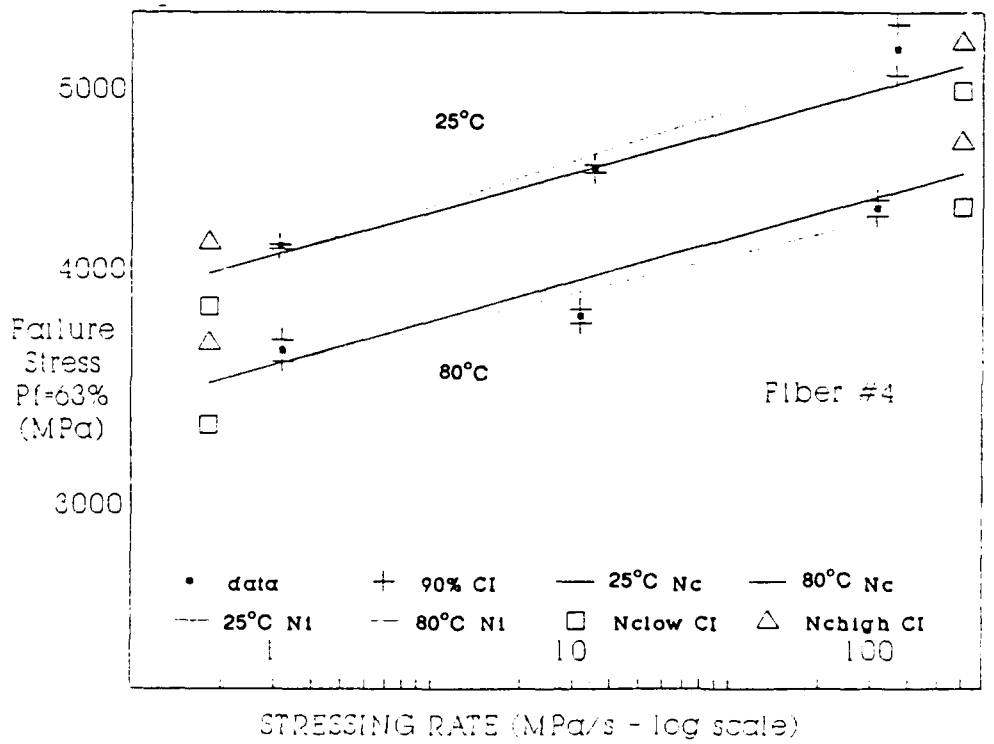

Figure 6d. Failure stress versus stress rate.

Table 3 values for E/[N+1], indicative of temperature sensitivity, confirm the observations of Weibull plots recorded in Table 2. Fibers 2, 3, and 4 exhibit similar sensitivity, contributing generally more than 10% strength loss from increasing test temperature from 25°C to 80°C; Fiber 1 lost less than 4% of its strength.

Table 3. DYNAMIC FATIGUE PARAMETERS

Fiber	N+1	E(kJ/mole)	B(MPa^2-s)	E/(N+1)	1nB 25°C	1nB 80°C
1	131(39)	51.8	1.05×10^{-04}	0.39	11.7(4.9)	8.5(5.9)
2	28.9(1.8)	53.5	4.23×10^{-04}	1.79	13.8(0.9)	10.5(1.1)
3	20.7(0.8)	41.3	3.24×10^{-02}	1.90	13.2(0.5)	10.7(0.7)
4	22.3(0.5)	47.9	1.42×10^{-02}	2.06	15.1(0.3)	12.1(0.4)

Standard deviations are expressed in parentheses.

Table 3 parameters are used to predict static fatigue behavior using the appropriate form of Equation 1. For pure static fatigue, solving for allowable applied stress results in the following equation:

$$S_a = [B' \exp(E/RT)\, S_i^{(N-2)} / t_f]^{1/N}. \quad (10)$$

Attempting to follow the France approximation for zero-stress aging, the strait line log-log plot of failure stress versus zero-stressed aging time fits a simpler equation quite well.

$$\ln S_{f(t)} = \ln S_x - b \ln(t) \quad (11)$$

Here, unaged strength, when t equals zero, must be approximated by the intercept value, S_x' when t equals 1 second. The France empirical equation (Equation 3), generated distinctly non linear plots for data in this study due to the ln(1+at) term. Any value of a results in two distinct regions on the curve. One region exists where 1 is much greater than the product at and dominates, and another exists where at is much greater than 1. The transition was inconsistent with the characteristic strength of the sample data here for any reasonable values of a and b. Extrapolated values for Pf equal 1% did seem to lend themselves to this transition, particularly for Fibers 1 and 3. These values fit in a more normal France equation.

$$\ln S_{f(t)} = \ln S_x - b \ln(1+at) \quad (12)$$

Using, for convenience, averaged data from the three stressing rates at the 1% probability of failure level, best-fit lines of the form (see Equations 11 and 12) were calculated. The data, calculated lines, and b values are shown in Figures 7a and 7b, Aging Behavior. A commonly acceptable value of 0.1 hr^{-1} was used for a. Fibers 1 and 3 have distinctive strength losses. Fibers 2 and 4 show very little change. This behavior was shown by France to be uniform for both dry and wet broken fiber, with simply an offset in intercept S_x, for samples taken from identically aged fiber. Calculations resulting from wet broken fiber should then be easily translated with replacement of S_x by S_i, the initial inert strength. Substitution of this representation of S_i into Equation 4 results in a modified static fatigue equation incorporating zero-stress aging effects.

$$S_a = [\{2B' \exp(E/RT)\{\exp[\ln S_i - b\ln(1+a*t_{f/2})]\}^{(N-2)}\} / t_f]^{1/N} \quad (13)$$

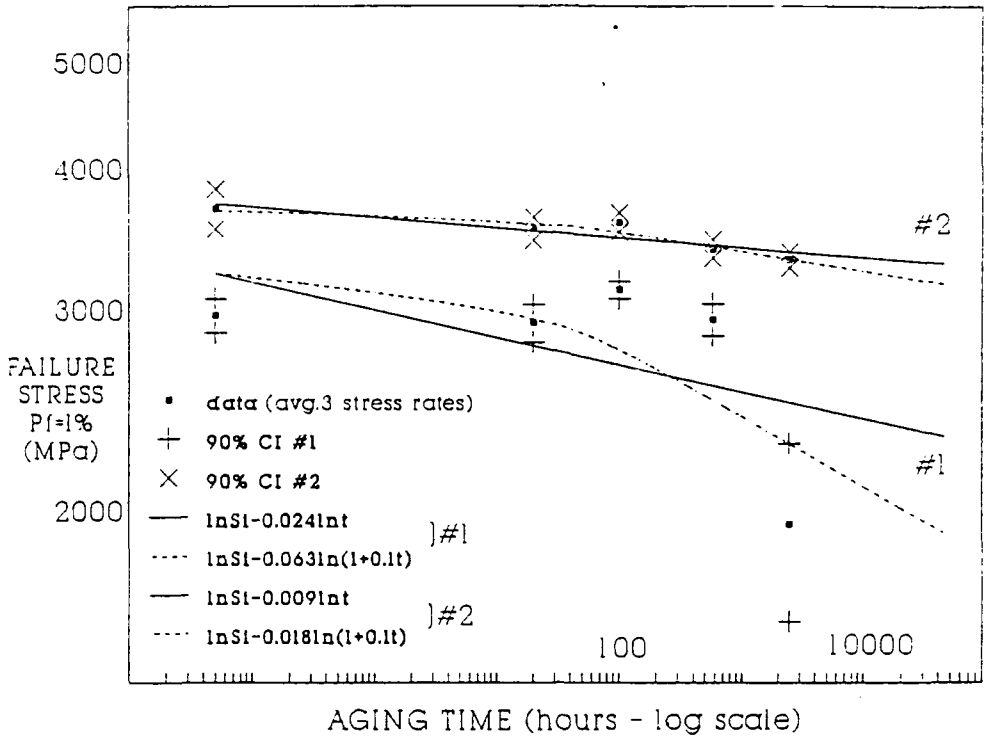

Figure 7a. Aging behavior Fibers 1 and 2.

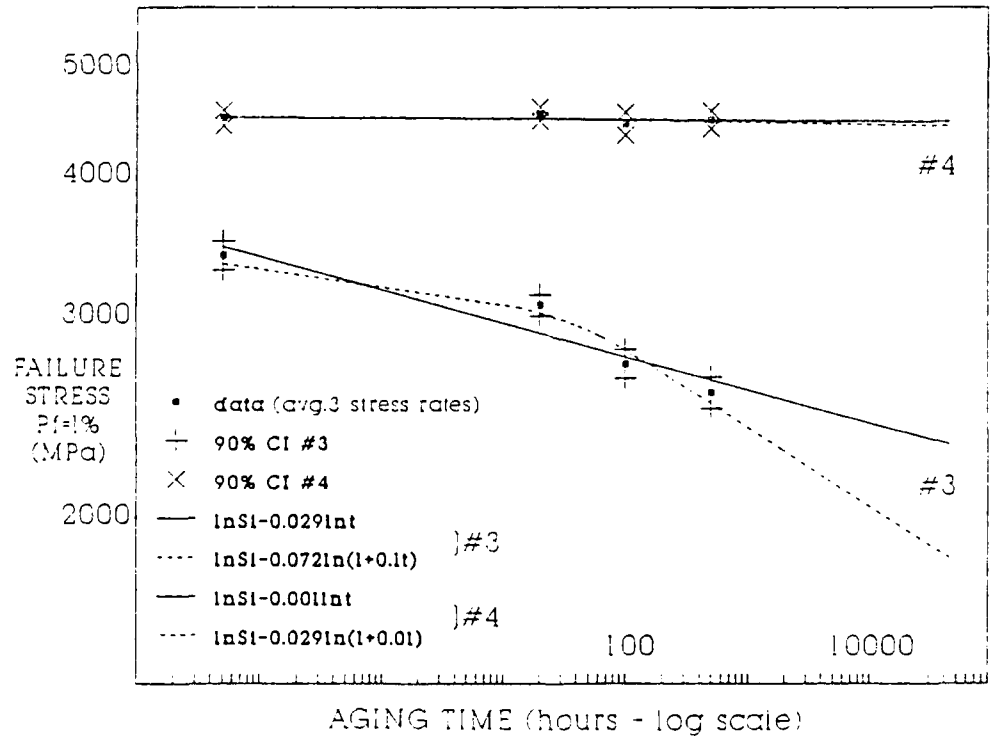

Figure 7b. Aging behavior Fibers 3 and 4.

Use of initial strength, S_i, values (estimated by the 1% probability of failure level for dry dynamic fatigue breaks at 100 MPa/s), and the dynamic fatigue parameters from Table 3 in Equations 10 and 13 produce Figure 8, Predicted Static Fatigue. It is important to note that the fatigue parameters used in both equations were derived from wet broken data, which is a worst-case scenario. The time-dependent behavior slopes, minus b, were derived from fiber aged in 65°C water, also a worst-case scenario. Therefore, it is logical to assume that the resultant predicted static fatigue behavior is for the worst case scenario, and the plots in Figure 8 can be interpreted as quite safe lower bounds for the 1% weak-strength tail of 0.1 meter samples.

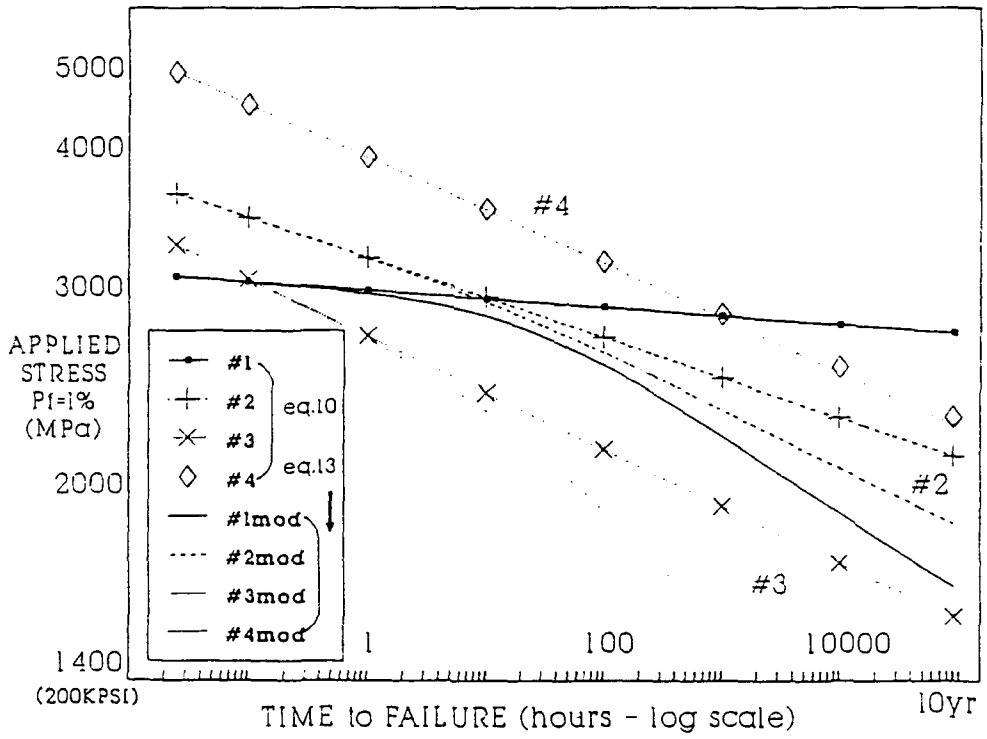

Figure 8. Predicted static fatigue.

It is quickly observed that although Fiber 1 has the lowest inert strength in this group, it quickly becomes dominant through strength retention and pure static fatigue resistance after one year. For modified static fatigue behavior Fiber 1 remains in the pack due to its strong zero-stress aging susceptibility. The right-hand calculated points for each line correspond to 10 years, a suggested shelf life for payout fiber applications. The 200 KPSI or 1380 MPa stress level commonly used in payout system design coincides with the abscissa axis to show the boundary of probable acceptance. Fiber 3 appears to be the only fiber unlikely to be unacceptable, but under pure static fatigue considerations is only marginal. This is consistent with the failure during aging of Fiber 3 under 1450 MPa bending stress at less than 212 hours, or approximately 0.025 year. This would seem to coincide reasonably well with the modified 4 line of Figure 8, supporting the accuracy of the model developed by France and modified analysis used here.

The amorphous carbon coating of Fiber 1 appears to succeed in desensitizing the fiber to static fatigue, but not zero-stress aging. Bimodal behavior evades this analysis somewhat, and the exceptional predicted static fatigue behavior of Fiber 1 is, therefore, relatively more generous than predicted behavior for Fibers 2 and 3. The bimodal behavior is probably the result of some processing impurity or other sporadic surface defect at the glass cladding/carbon interface, or quite possible, a thinning of the coating. Typical hermetic coatings are very thin, 50 to 500 angstroms, and more difficult to monitor and control than glass fiber and polymer buffer thicknesses one thousand times greater. Uniformity has improved dramatically since successful demonstration of fiber optics in the 1970s, and application of vapor deposition coating techniques to fiber optics in the 1980s.

Hermetically coated Fiber 2 fares slightly better than Fibers 3 and 4 in pure static fatigue prediction, but suffers significantly from zero-stress aging, unlike Fiber 4.

SUMMARY

Overall, the four optical fibers tested have tightly grouped Weibull distributions with moduli in excess of 40, and fatigue parameters N greater than 20, or above average. Fiber 1 has high dynamic fatigue resistance and high aging resistance at characteristic strength levels. The slightly low initial inert strength and inconsistent bimodal behavior are the only drawbacks to this fiber. Fiber 2 has balanced properties of good initial strength, fatigue resistance, and aging resistance. Fiber 4 has high initial strength and high aging resistance but fair fatigue resistance. Fibers 1, 2, and 4 appear completely reliable for design strength in excess of 10 years. Fiber 3 is marginally acceptable, dependent upon the accuracy of the modified static fatigue analysis used here. Hermetic-coated fiber does demonstrate a marginal advantage over simple high strength or passivating polymer-coated fiber.

ACKNOWLEDGMENTS

This study was partially supported by the U.S. Army Missile Command under MIPR No. W81E54EC25.

The author wishes to thank George D. Quinn for his frequent input on the statistical treatments of mechanical testing data and their relative significance at low strength and probability tails, and to Michael J. Slavin for his consistent support of this effort in administrative detail, technical suggestions, and personal energy.

The author also wishes to thank AT&T, c/o Albert Konchar, Jr., Guilford Center, PO Box 20046, Greensboro, NC 27420-0046; Corning Glass Works, c/o James C. Vernon, Telecommunications Products Division, Advanced Fiber Products Department, CGW BH3, Corning, NY 14831; Ensign Bickford, c/o Joseph Burke, 16-18 Ensign Drive, Avon, CT 06001; and GTE Labs, c/o Dr. Michael Wei, 40 Sylvan Road, Waltham, MA 02154.

APPENDIX A

Table A1a. DYNAMIC FATIGUE RESULTS FOR FIBER 1

Test Conditions			Weibull Parameters			Average Strength (MPa)	
Temp (T) (°C)	S Rate (MPa/s)	Sample Size	Slope m	S_o (MPa)	$\ln(S_o)$	S_f Avg	Std Dev
25-d	93.7	20	66	3460	8.149	3432	62
80	97.6	18	47	3267	8.092	3229	77
80	9.6	20	57	3249	8.086	3217	66
80	1.35	20	35	3175	8.063	3126	105
25	99	20	15	3394	8.130	3275	212
25	14	20	64	3340	8.114	3312	61
25	1.42	20	41	3269	8.092	3226	86

Table A1b. DYNAMIC FATIGUE RESULTS FOR AGED FIBER 1

Aging Conditions		Test Conditions		Weibull Parameters			Average Strength (MPa)	
Time (t) (Hr)	Stress (MPa)	S Rate (MPa/s)	Sample Size	Slope m	S_o (MPa)	$\ln(S_o)$	S_f Avg	Std Dev
20.16	70-b	114.3	20	27	3373	8.124	3306	132
20.16	70-b	13.7	20	21	3362	8.120	3275	146
20.16	70-b	1.53	20	60	3255	8.088	3225	64
100	70-b	102.7	20	105	3358	8.119	3340	37
100	70-b	13.8	20	81	3303	8.103	3280	47
100	70-b	1.5	20	55	3294	8.100	3261	69
572	70-b	105.9	20	59	3328	8.110	3297	64
572	70-b	10.7	20	32	3303	8.103	3248	109
572	70-b	1.42	20	37	3231	8.081	3183	94
2450	70-b	124.4	20	7	3345	8.115	3130	426
2450	70-b	10.5	20	10	3309	8.105	3150	291
2450	70-b	0.78	7	9	3163	8.059	2994	360
44	1450-b	109.5	21	41	3395	8.130	3350	84
44	1450-b	12.06	20	92	3354	8.118	3333	43
44	1450-b	1.5	6	11	3265	8.091	3120	268
212	1450-b	107.9	20	52	3388	8.128	3352	68
212	1450-b	10.27	20	10	3412	8.135	3245	262
212	1450-b	1.48	18	81	3312	8.105	3289	48
1052	1450-b	112.6	20	56	3447	8.145	3413	69
1052	1450-b	11.02	20	94	3388	8.128	3368	42
1052	1450-b	1.34	20	94	3306	8.104	3287	41
24	340-t	98	5	94	3374	8.124	3355	35
24	340-t	73.7	7	105	3372	8.123	3355	33
190	340-t	9.83	10	150	3356	8.119	3344	25
190	340-t	8.98	10	76	3379	8.125	3355	47

Table A2a. DYNAMIC FATIGUE RESULTS FOR FIBER 2

Test Conditions			Weibull Parameters			Average Strength (MPa)	
Temp (T) (°C)	S Rate (MPa/s)	Sample Size	Slope m	S_o (MPa)	$\ln(S_o)$	S_f Avg	Std Dev
25-d	93.6	20	61	4989	8.515	4943	93
80	103.4	17	120	3861	8.259	3843	38
80	9.86	20	116	3474	8.153	3457	35
80	1.0	20	17	3362	8.120	3259	200
25	89.9	14	45	4347	8.377	4295	108
25	9.2	20	9	4310	8.368	4053	415
25	1.06	3	79	3635	8.198	3613	39

Table A2b. DYNAMIC FATIGUE RESULTS FOR AGED FIBER 2

Aging Conditions		Test Conditions		Weibull Parameters			Average Strength (MPa)	
Time (t) (Hr)	Stress (MPa)	S Rate (MPa/s)	Sample Size	Slope m	S_o (MPa)	$\ln(S_o)$	S_f Avg	Std Dev
20.16	70-b	100.6	20	71	4205	8.344	4173	60
20.16	70-b	10.5	20	82	3783	8.238	3757	53
20.16	70-b	0.85	9	40	3434	8.142	3388	91
100	70-b	96.5	5	101	4133	8.327	4111	42
100	70-b	11.2	20	72	3770	8.235	3741	59
100	70-b	0.91	17	81	3475	8.153	3451	50
572	70-b	85.4	20	68	3929	8.301	3897	65
572	70-b	10.8	19	82	3607	8.191	3583	50
572	70-b	1.0	14	82	3298	8.101	3276	47
2450	70-b	102.9	20	47	3870	8.261	3825	95
2450	70-b	10.2	21	107	3517	8.165	3498	37
2450	70-b	1.01	19	96	3175	8.063	3156	38
44	1450-b	134.9	16	64	4277	8.361	4240	78
44	1450-b	11.19	15	68	3791	8.241	3761	62
44	1450-b	1.19	8	89	3483	8.156	3461	36
212	1450-b	116.1	17	83	4131	8.326	4104	57
212	1450-b	12.12	18	63	3784	8.239	3751	68
212	1450-b	1.24	10	99	3509	8.163	3490	40
1052	1450-b	119.5	11	52	4444	8.399	4398	95
1052	1450-b	12.89	11	69	3843	8.254	3813	62
1052	1450-b	1.54	11	98	3424	8.139	3405	34
24	22	108.2	10	139	4270	8.359	4253	34
24	202	10.9	10	82	3781	8.238	3756	51
24	2002	1.25	7	89	3402	8.132	3381	40
190	302	8.89	9	11	3665	8.207	3500	265

Table A3a. DYNAMIC FATIGUE RESULTS FOR FIBER 3

Test Conditions			Weibull Parameters			Average Strength (MPa)	
Temp (T) (°C)	S Rate (MPa/s)	Sample Size	Slope m	S_o (MPa)	$\ln(S_o)$	S_f Avg	Std Dev
25-d	79.2	20	59	5068	8.531	5021	101
80	100.5	19	81	3370	8.123	3347	49
80	9.17	20	92	3047	8.022	3029	39
80	0.88	19	18	2857	7.958	2770	145
25	108.3	20	46	4440	8.398	4388	112
25	4.73	19	59	3548	8.171	3515	69
25	0.42	12	48	3071	8.030	3036	71

Table A3b. DYNAMIC FATIGUE RESULTS FOR AGED FIBER 3

Aging Conditions		Test Conditions		Weibull Parameters			Average Strength (MPa)	
Time (t) (Hr)	Stress (MPa)	S Rate (MPa/s)	Sample Size	Slope m	S_o (MPa)	$\ln(S_o)$	S_f Avg	Std Dev
20	70-b	92.9	20	57	3755	8.231	3720	77
20	70-b	9.06	20	82	3229	8.080	3207	45
20	70-b	0.65	19	52	2823	7.945	2793	62
100	70-b	87.0	20	39	3345	8.115	3298	98
100	70-b	8.79	20	67	2981	8.000	2957	50
100	70-b	0.83	19	36	2607	7.866	2569	82
500	70-b	79.0	20	36	3196	8.070	3149	100
500	70-b	9.64	20	55	2836	7.950	2808	58
500	70-b	0.79	18	38	2478	7.815	2443	75
44	1450-b	123.9	20	33	3388	8.128	3332	120
44	1450-b	9.72	20	27	3023	8.014	2964	127
44	1450-b	1.0	21	35	2679	7.893	2638	88
24	340-t	87.5	12	17	3364	8.121	3265	212
24	340-t	9.36	10	18	2896	7.971	2815	169
190	340-t	10.69	12	13	3033	8.017	2912	242

Table A4a. DYNAMIC FATIGUE RESULTS FOR FIBER 4

Test Conditions			Weibull Parameters			Average Strength (MPa)	
Temp (T) (°C)	S Rate (MPa/s)	Sample Size	Slope m	S_o (MPa)	$\ln(S_o)$	S_f Avg	Std Dev
25-d	109.9	20	121	5869	8.678	5842	54
80	103.8	20	44	4380	8.385	4326	97
80	10.47	20	52	3831	8.251	3790	81
80	1.05	22	31	3666	8.207	3602	115
25	121.5	20	14	5347	8.584	5145	305
25	11.7	20	84	4601	8.444	4570	63
25	1.03	19	157	4171	8.336	4156	31

Table A4b. DYNAMIC FATIGUE RESULTS FOR AGED FIBER 4

Aging Conditions		Test Conditions		Weibull Parameters			Average Strength (MPa)	
Time (t) (Hr)	Stress (MPa)	S Rate (MPa/s)	Sample Size	Slope m	S_o (MPa)	$\ln(S_o)$	S_f Avg	Std Dev
23.16	70-b	109.8	20	80	5327	8.581	5290	78
23.16	70-b	10.8	20	111	4611	8.436	4588	47
23.16	70-b	0.99	20	105	4199	8.343	4176	45
100	70-b	99.6	19	64	5354	8.586	5308	94
100	70-b	11.6	20	69	4788	8.474	4750	74
100	70-b	0.99	20	43	4171	8.336	4119	106
503.16	70-b	98.8	20	113	5312	8.578	5286	55
503.16	70-b	10.7	20	15	4698	8.455	4536	278
503.16	70-b	1.01	20	93	4182	8.339	4157	53
44	1450-b	125.2	20	72	5144	8.546	5105	81
44	1450-b	11.27	19	82	4499	8.412	4468	63
44	1450-b	1.11	11	87	4065	8.310	4040	51
212	1450-b	116.3	16	47	5404	8.595	5342	126
212	1450-b	11.79	16	24	4965	8.510	4853	211
212	1450-b	1.1	20	36	4286	8.363	4221	122
1052	1450-b	119.5	20	36	5079	8.533	5003	164
1052	1450-b	12	22	29	4698	8.455	4611	188
1052	1450-b	1.34	9	30	4322	8.371	4245	162
190	340-t	99.4	20	11	5910	8.684	5634	435
190	340-t	9.96	20	25	5227	8.562	5116	195
190	340-t	0.95	10	54	4433	8.397	4389	92

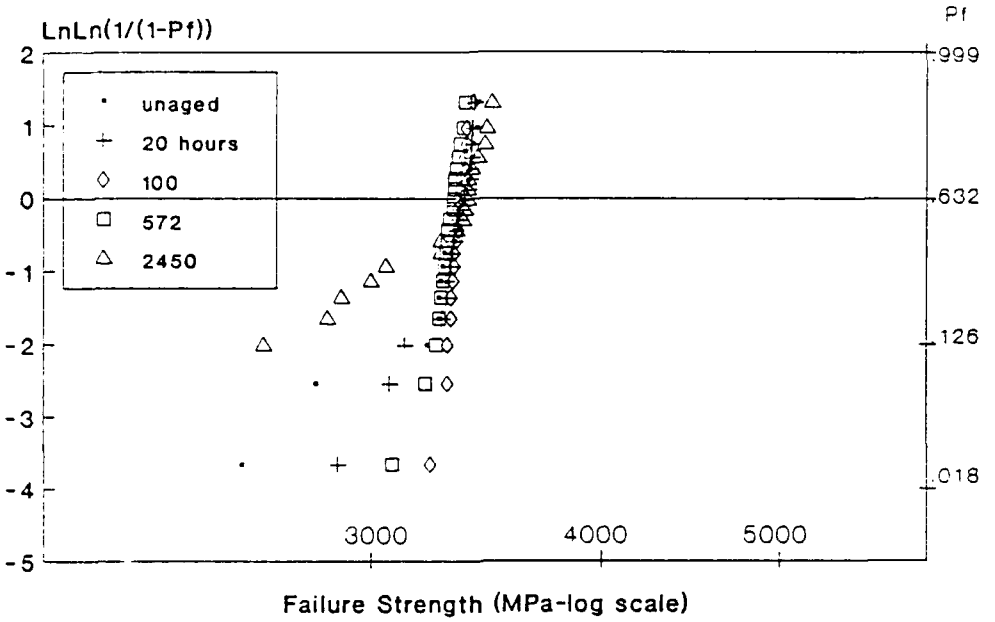

aged 65°C in water

Figure A1. Aged breaking strength Weibull plots Fiber 1 (100 MPa/s).

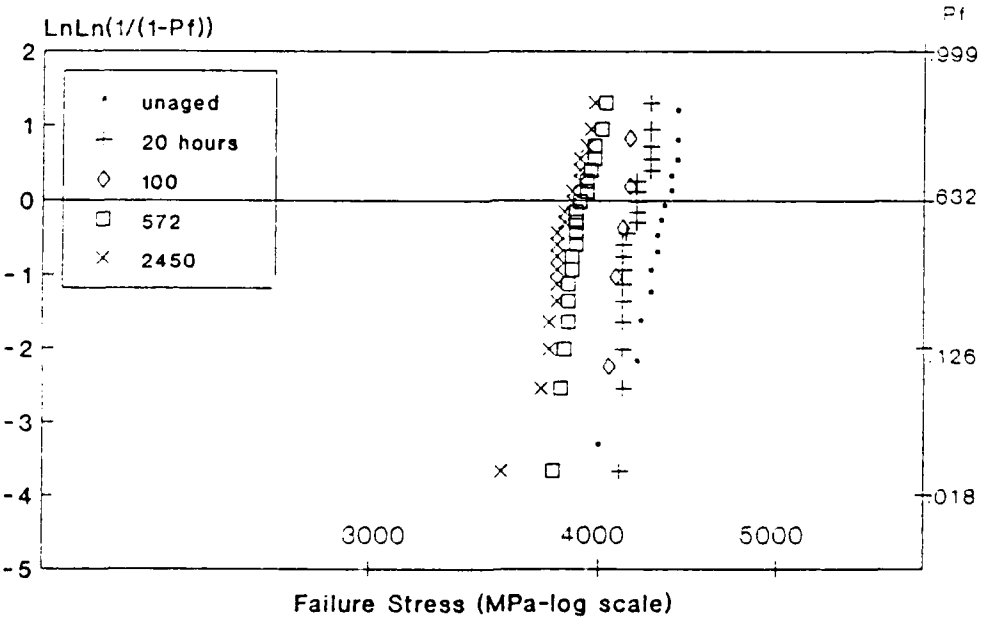

aged 65°C in water

Figure A2. Aged breaking strength Weibull plots Fiber 2 (100 MPa/s).

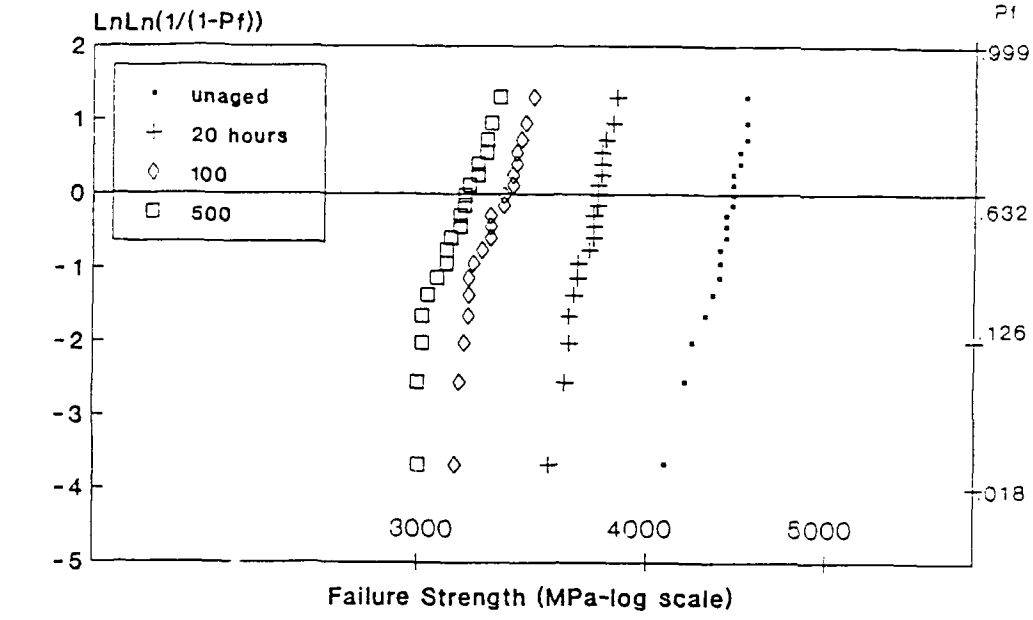

Figure A3. Aged breaking strength Weibull plots Fiber 3 (100 MPa/s).

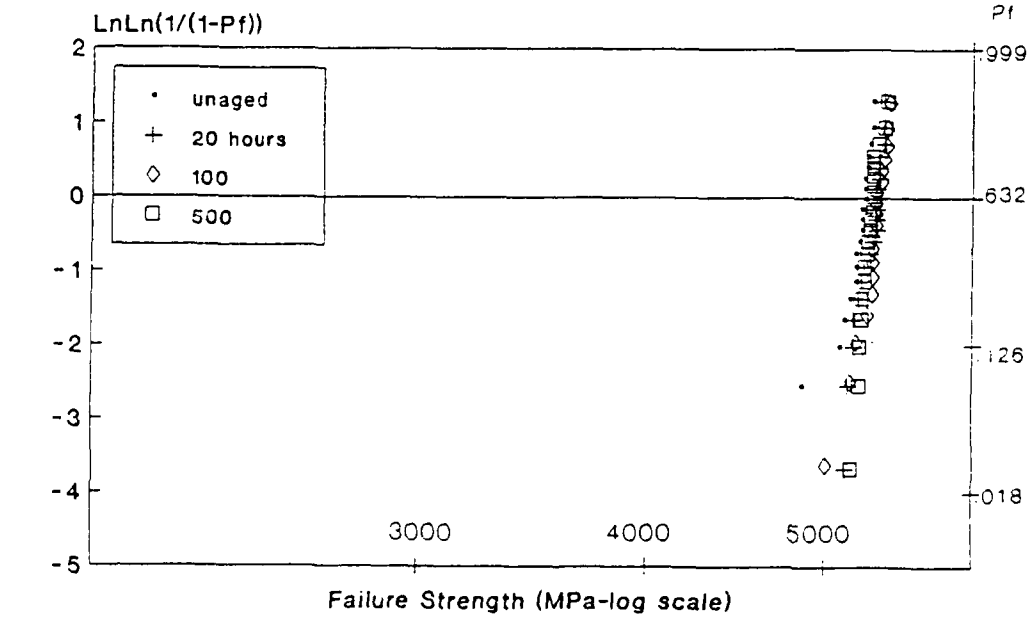

Figure A4. Aged breaking strength Weibull plots Fiber 4 (100 MPa/s).

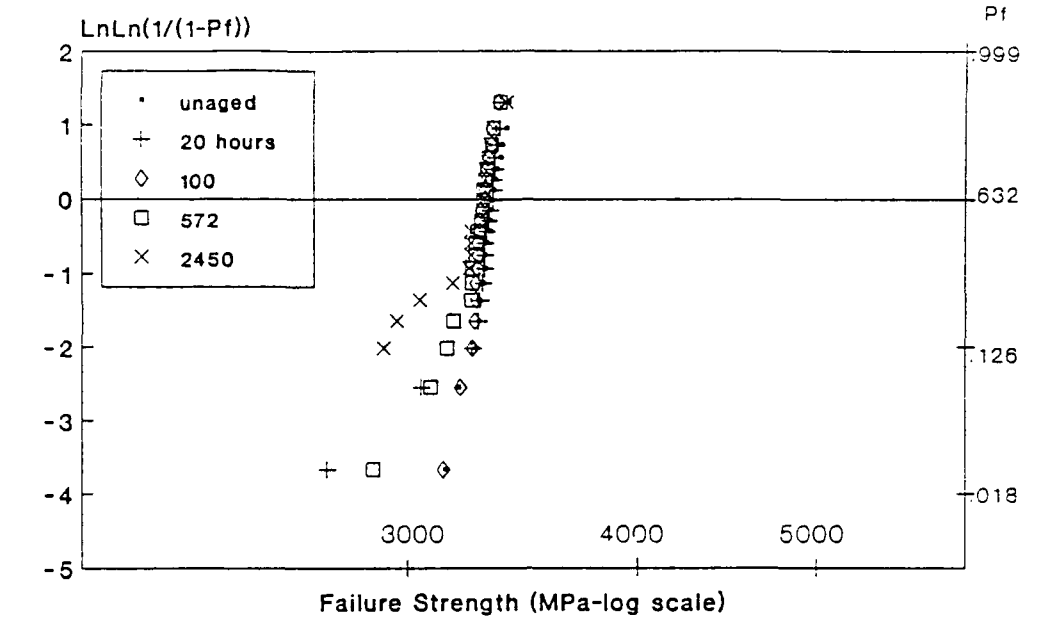

Figure A5. Aged breaking strength Weibull plots Fiber 1 (10 MPa/s).

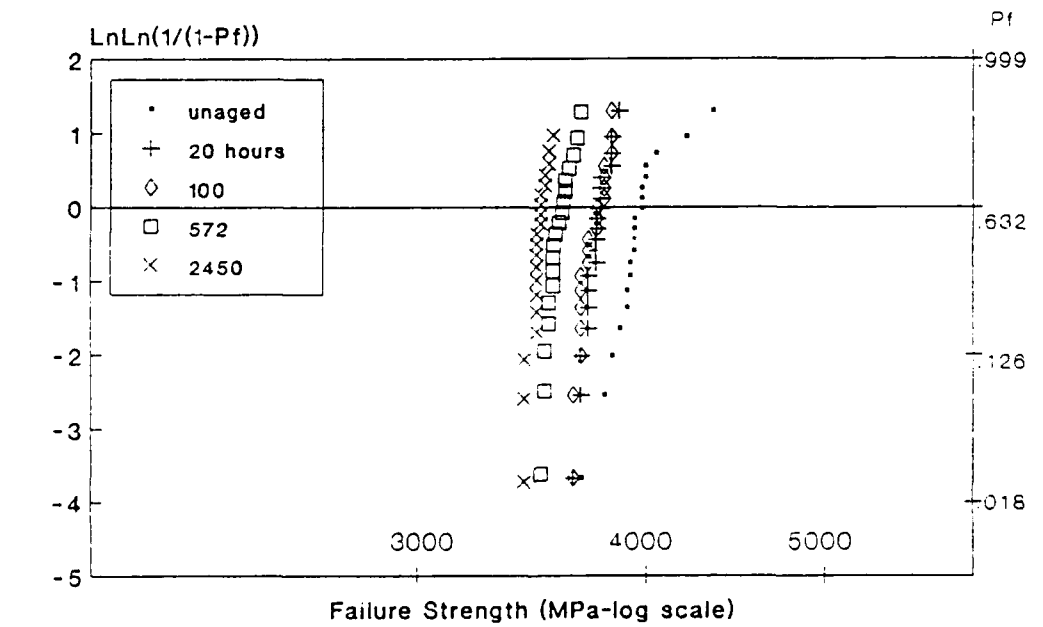

Figure A6. Aged breaking strength Weibull plots Fiber 2 (10 MPa/s).

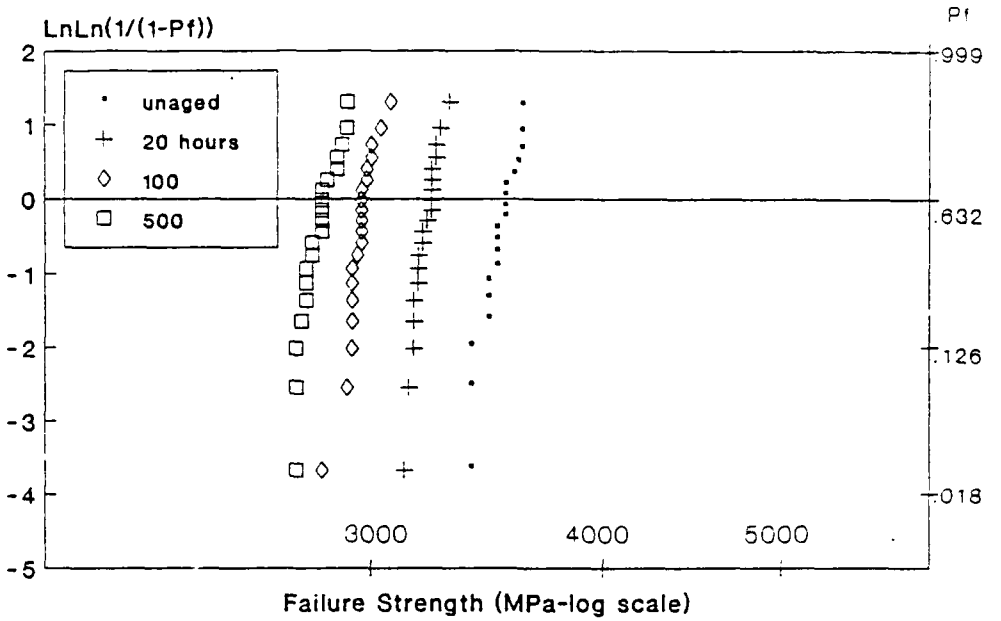

aged 65°C in water

Figure A7. Aged breaking strength Weibull plots Fiber 3 (10 MPa/s).

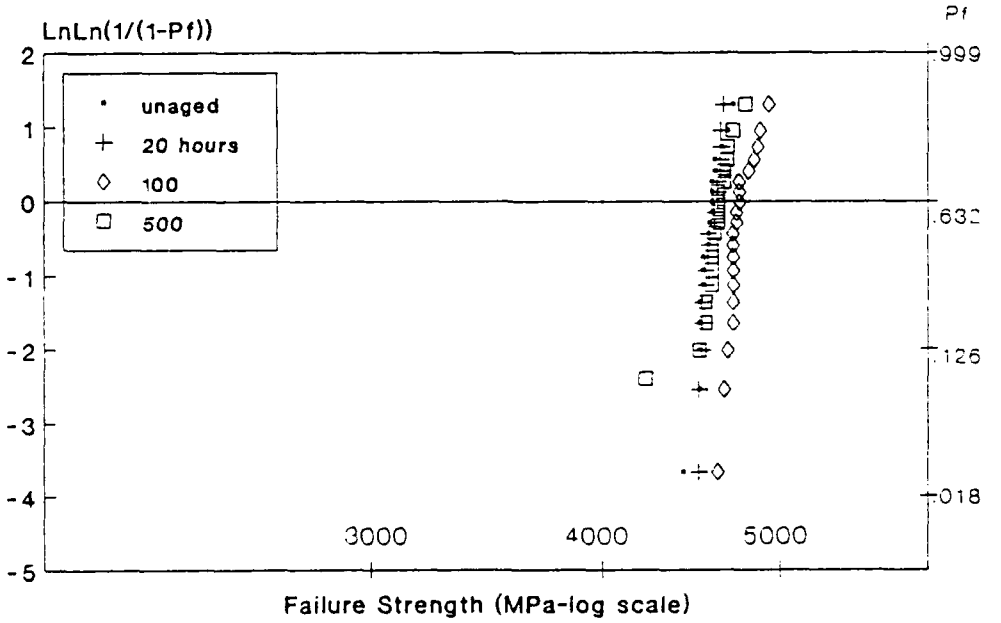

aged 65°C in water

Figure A8. Aged breaking strength Weibull plots Fiber 4 (10 MPa/s).

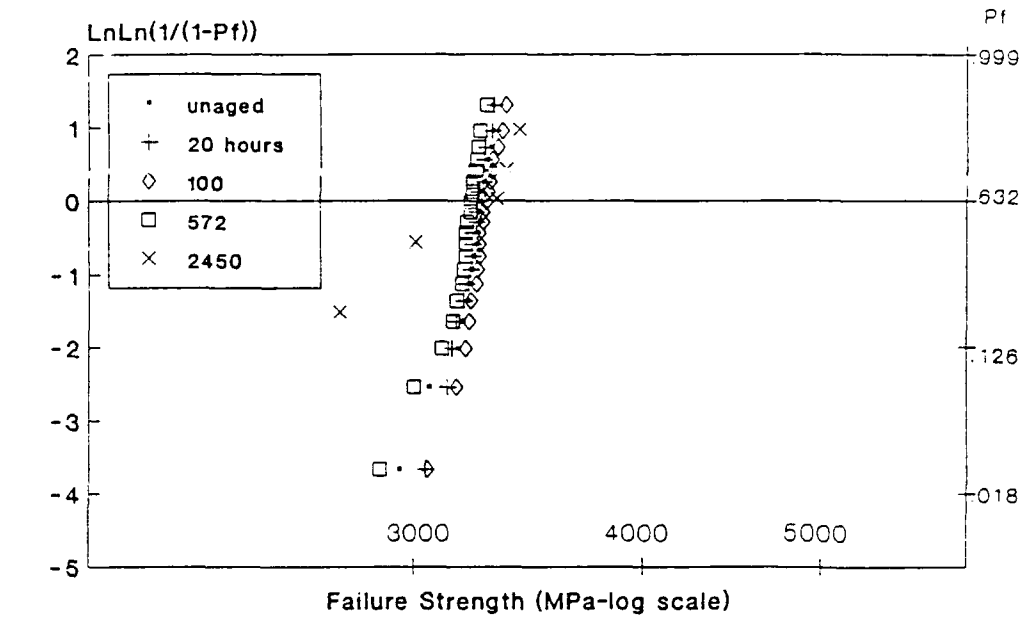

aged 65°C in water

Figure A9. Aged breaking strength Weibull plots Fiber 1 (1 MPa/s).

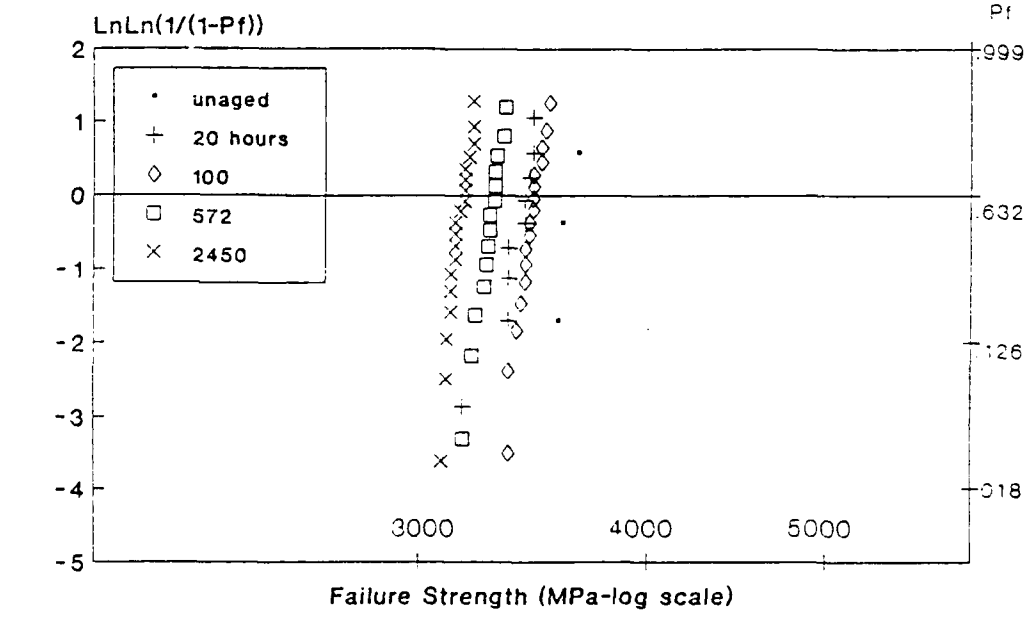

aged 65°C in water

Figure A10. Aged breaking strength Weibull plots Fiber 2 (1 MPa/s).

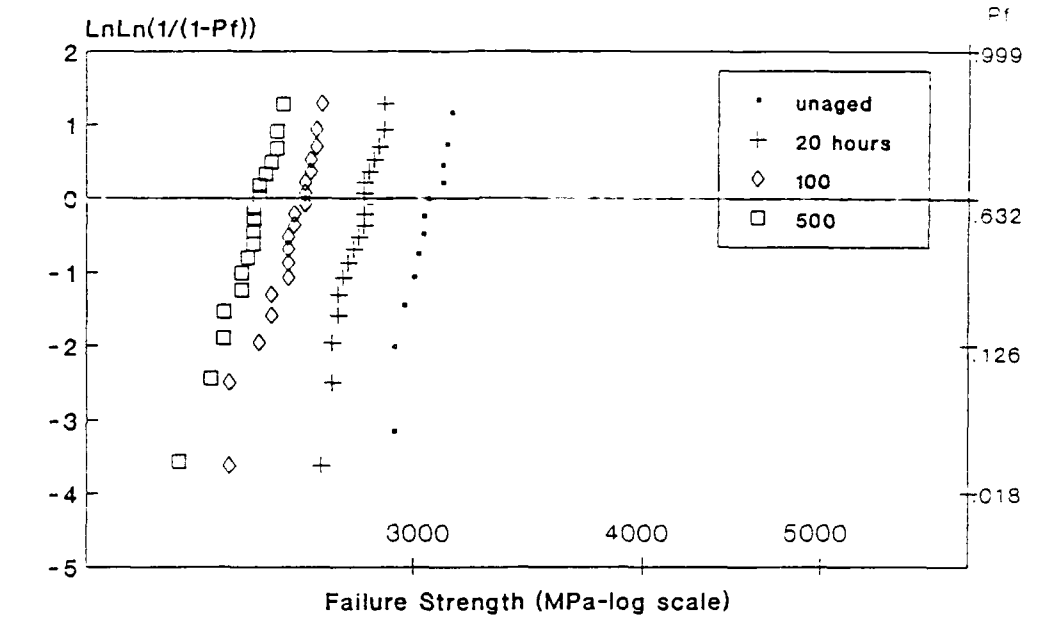

Figure A11. Aged breaking strength Weibull plots Fiber 3 (1 MPa/s).

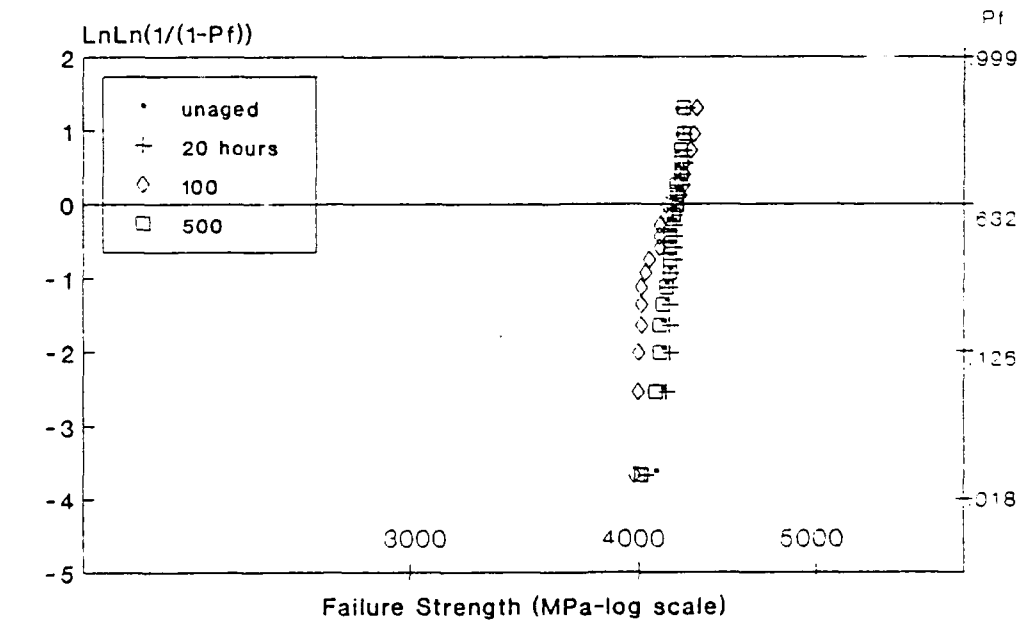

Figure A12. Aged breaking strength Weibull plots Fiber 4 (1 MPa/s).

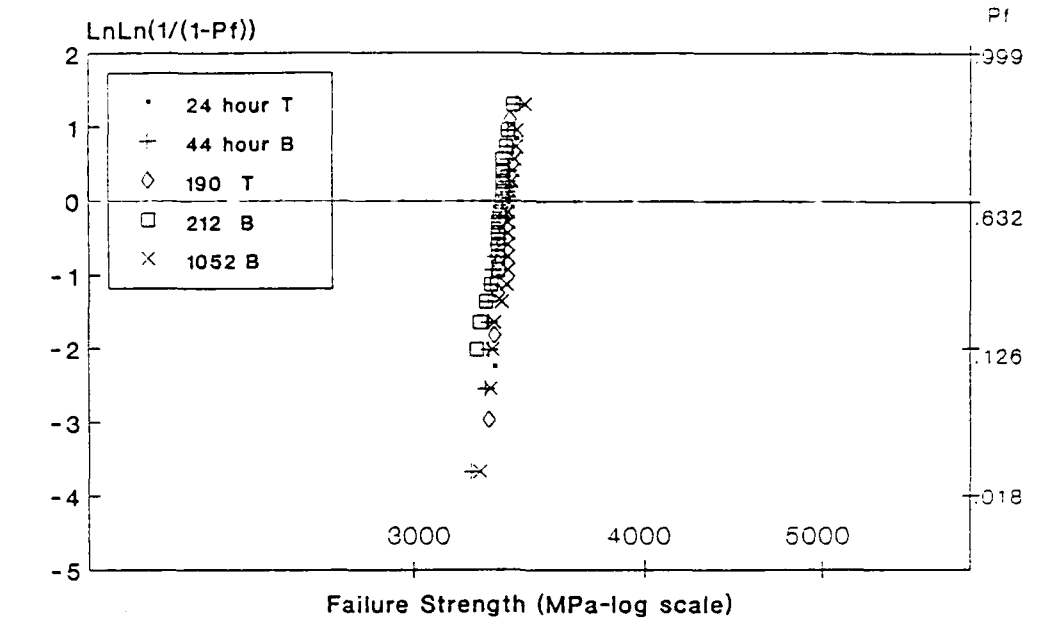

Figure A13. Stress aged strength Weibull plots Fiber 1 (10 MPa/s).

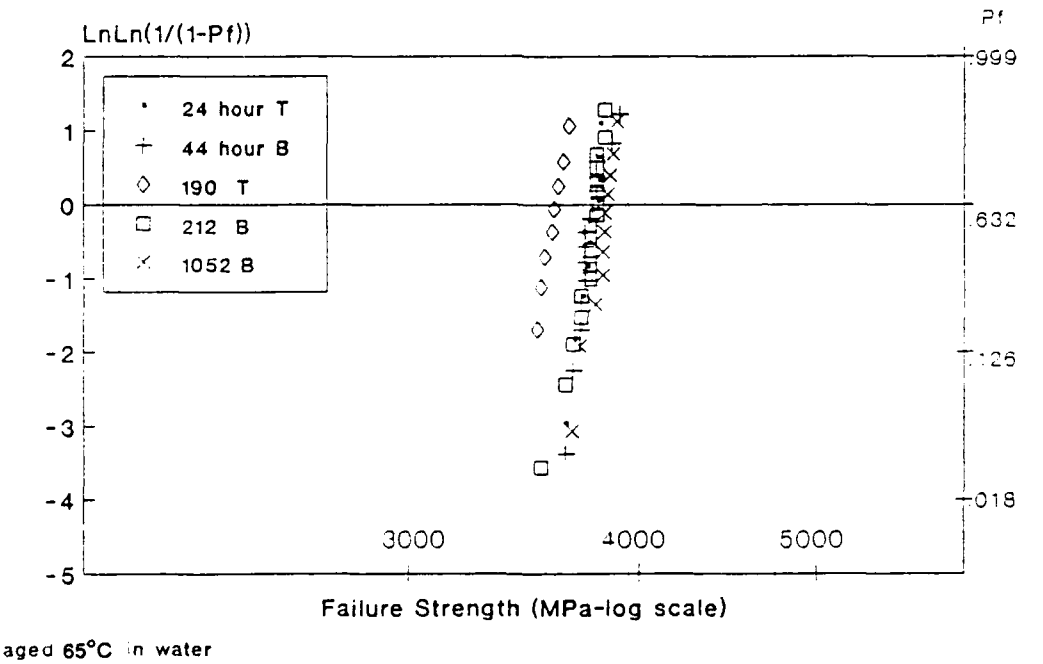

Figure A14. Stress aged strength Weibull plots Fiber 2 (10 MPa/s).

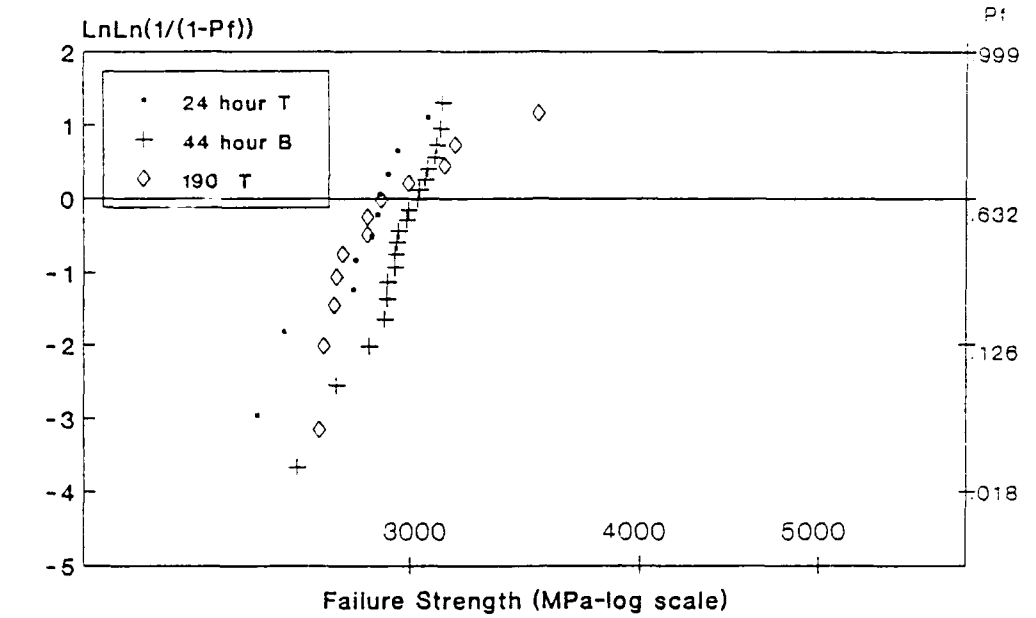

aged 65°C in water

Figure A15. Stress aged strength Weibull plots Fiber 3 (10 MPa/s).

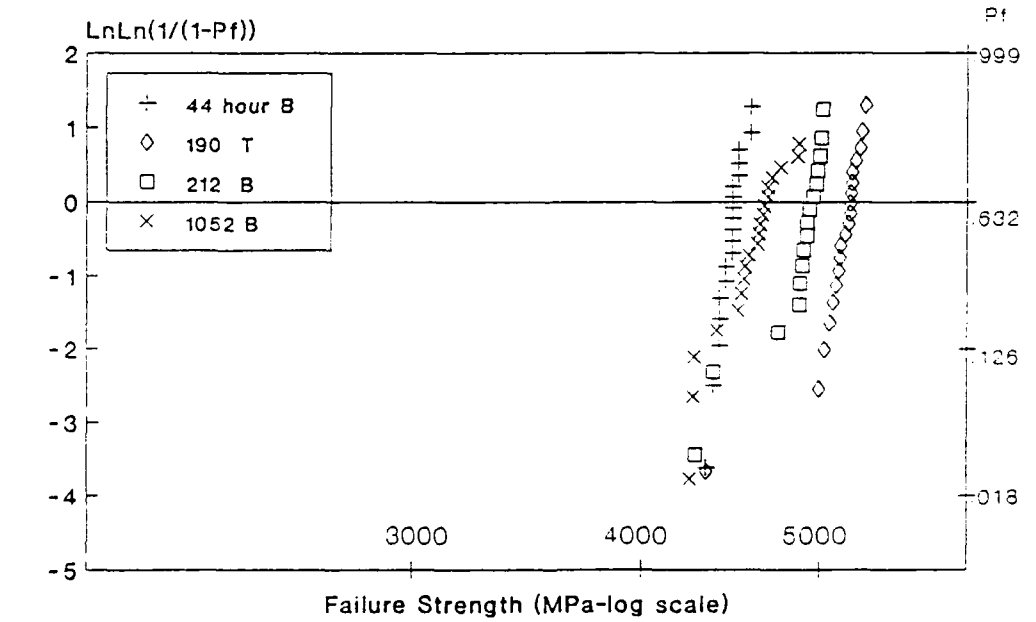

aged 65°C in water

Figure A16. Stress aged strength Weibull plots Fiber 4 (10 MPa/s).

DISTRIBUTION LIST

No. of Copies	To
1	Office of the Under Secretary of Defense for Research and Engineering, The Pentagon, Washington, DC 20301
	Commander, U.S. Army Laboratory Command, 2800 Powder Mill Road, Adelphi, MD 20783-1145
1	ATTN: AMSLC-IM-TL
1	AMSLC-CT
	Commander, Defense Technical Information Center, Cameron Station, Building 5, 5010 Duke Street, Alexandria, VA 22304-6145
2	ATTN: DTIC-FDAC
1	MIAC/CINDAS, Purdue University, 2595 Yeager Road, West Lafayette, IN 47905
	Commander, Army Research Office, P.O. Box 12211, Research Triangle Park, NC 27709-2211
1	ATTN: Information Processing Office
	Commander, U.S. Army Materiel Command, 5001 Eisenhower Avenue, Alexandria, VA 22333
1	ATTN: AMCSCI
	Commander, U.S. Army Materiel Systems Analysis Activity, Aberdeen Proving Ground, MD 21005
1	ATTN: AMXSY-MP, H. Cohen
	Commander, U.S. Army Missile Command, Redstone Scientific Information Center, Redstone Arsenal, AL 35898-5241
1	ATTN: AMSMI-RD-CS-R/Doc
1	AMSMI-RLM
	Commander, U.S. Army Armament, Munitions and Chemical Command, Dover, NJ 07801
2	ATTN: Technical Library
1	AMDAR-LCA, Mr. Harry E. Pebly, Jr., PLASTEC, Director
	Commander, U.S. Army Natick Research, Development and Engineering Center, Natick, MA 01760-5010
1	ATTN: Technical Library
	Commander, U.S. Army Satellite Communications Agency, Fort Monmouth, NJ 07703
1	ATTN: Technical Document Center
	Commander, U.S. Army Tank-Automotive Command, Warren, MI 48397-5000
1	ATTN: AMSTA-ZSK
2	AMSTA-TSL, Technical Library
	Commander, White Sands Missile Range, NM 38002
1	ATTN: STEWS-WS-VT
	President, Airborne, Electronics and Special Warfare Board, Fort Bragg, NC 28307
1	ATTN: Library
	Director, U.S. Army Ballistic Research Laboratory, Aberdeen Proving Ground, MD 21005
1	ATTN: SLCBR-TSB-S (STINFO)
	Commander, Dugway Proving Ground, Dugway, UT 84022
1	ATTN: Technical Library, Technical Information Division
	Commander, Harry Diamond Laboratories, 2800 Powder Mill Road, Adelphi, MD 20783
1	ATTN: Technical Information Office
	Director, Benet Weapons Laboratory, LCWSL, USA AMCCOM, Watervliet, NY 12189
1	ATTN: AMSMC-LCB-TL
1	AMSMC-LCB-R
1	AMSMC-LCB-RM
1	AMSMC-LCB-RP
	Commander, U.S. Army Foreign Science and Technology Center, 220 7th Street, N.E., Charlottesville, VA 22901-5396
3	ATTN: AIFRTC, Applied Technologies Branch, Gerald Schlesinger

No. of Copies	To
	Commander, U.S. Army Aeromedical Research Unit, P.O. Box 577, Fort Rucker, AL 36360
1	ATTN: Technical Library
	Commander, U.S. Army Aviation Systems Command, Aviation Research and Technology Activity, Aviation Applied Technology Directorate, Fort Eustis, VA 23604-5577
1	ATTN: SAVDL-E-MOS
	U.S. Army Aviation Training Library, Fort Rucker, AL 36360
1	ATTN: Building 5906-5907
	Commander, U.S. Army Agency for Aviation Safety, Fort Rucker, AL 36362
1	ATTN: Technical Library
	Commander, USACDC Air Defense Agency, Fort Bliss, TX 79916
1	ATTN: Technical Library
	Commander, U.S. Army Engineer School, Fort Belvoir, VA 22060
1	ATTN: Library
	Commander, U.S. Army Engineer Waterways Experiment Station, P. O. Box 631, Vicksburg, MS 39180
1	ATTN: Research Center Library
	Commandant, U.S. Army Quartermaster School, Fort Lee, VA 23801
1	ATTN: Quartermaster School Library
	Naval Research Laboratory, Washington, DC 20375
1	ATTN: Code 5830
2	Dr. G. R. Yoder - Code 6384
	Chief of Naval Research, Arlington, VA 22217
1	ATTN: Code 471
1	Edward J. Morrissey, WRDC/MLTE, Wright-Patterson Air Force, Base, OH 45433-6523
	Commander, U.S. Air Force Wright Research & Development Center, Wright-Patterson Air Force Base, OH 45433-6523
1	ATTN: WRDC/MLLP, M. Forney, Jr.
1	WRDC/MLBC, Mr. Stanley Schulman
	NASA - Marshall Space Flight Center, MSFC, AL 35812
1	ATTN: Mr. Paul Schuerer/EH01
	U.S. Department of Commerce, National Institute of Standards and Technology, Gaithersburg, MD 20899
1	ATTN: Stephen M. Hsu, Chief, Ceramics Division, Institute for Materials Science and Engineering
1	Committee on Marine Structures, Marine Board, National Research Council, 2101 Constitution Ave., N.W., Washington, DC 20418
1	Librarian, Materials Sciences Corporation, 930 Harvest Drive, Suite 300, Blue Bell, PA 19422
1	The Charles Stark Draper Laboratory, 68 Albany Street, Cambridge, MA 02139
	Wyman-Gordon Company, Worcester, MA 01601
1	ATTN: Technical Library
	Lockheed-Georgia Company, 86 South Cobb Drive, Marietta, GA 30063
1	ATTN: Materials and Processes Engineering Dept. 71-11, Zone 54
	General Dynamics, Convair Aerospace Division, P.O. Box 748, Fort Worth, TX 76101
1	ATTN: Mfg. Engineering Technical Library

No. of Copies	To
	Spectran Corp. 50 Hall Road, Sturbridge, MA 01566
1	ATTN: Dr. Dipak Biswas
1	Lubos Vacha
	Ensign Bickford, 16 Ensign Drive, Avon, CT 06001
1	ATTN: Joe Burke
1	J. P. Clarkin
1	Bolesh J. Skutnik
	AT&T, 2000 Northeast Expressway, Norcross, GA 30071
1	ATTN: Laurie T. Carlton
1	Thomas Chapin
1	Charlie Jackson
1	Mickey R. Reynolds
1	David J. Voss
	Department of the Navy, Anti-Sub. Sys. Proj., Washington, DC 20362
1	ATTN: Ariadne, CDR Kirk E. Evans
1	Ariadne, Dr. George Hetland, Jr.
	Corning Glass Works, Corning, NY 14831
1	ATTN: Dr. Suresh T. Gulati, Res. & Dev. Division
1	Michael K. Reunert, MP-RO-03-1
1	Tim Starkey, BH-3
1	James Vernon, BH-3
	Commander, U.S. Army Missile Command, Redstone Scientific Information Center, Redstone Arsenal, AL 35898-5241
1	ATTN: AMSMI-RGT, Dr. Paul Jacobs
1	AMSMI-RGT, Dr. Paul Ruffin
	U.S. Army CECOM, Fort Monmouth, NJ 07703
1	ATTN: AMSEL-COM-RM-1, Dr. Vasilios Kalomiris
1	Kamran Karbassiyoon, ALCATEL, 7635 Plantation Road, Roanoke, VA 24019
1	Al Konchar, Guilford Center, P.O. Box 20046, Greensboro, NC 27420-0046
	Naval Underwater Systems Center, New London, CT 06320
1	ATTN: Patricia Kurdzial
1	Dr. Charles R. Kurkjian, 600 Mountain Avenue, Room 1A318, Murray Hill, NJ 07974
1	A. D. Morrison, JPL, CIT, 4800 Oak Grove Drive, Pasadena, CA 91109
	Naval Ocean Sys. Cen., P.O. Box 997, Kailua, HI 96734
1	ATTN: Code 5332, Dr. Arthur Nakagawa
	Naval Ocean Sys. Cen., San Diego, CA 92152
1	ATTN: Code 562, Dr. Howard Rast
1	Dr. John Ritter, Univ. of Massachusetts, Mechanical Engineering Dept., 12A Marston Hall, Amherst, MA 01003
	Naval Weapons Center, China Lake, CA 93555
1	ATTN: Edward Scullin
	NRL, Optical Techniques Branch, Washington, DC 20375
1	ATTN: Code 6573, Dr. George Sigel, Jr.
1	Dr. Michael Wei, GTE Labs, 40 Sylvan Road, Waltham, MA 02154
	Director, U.S. Army Materials Technology Laboratory, Watertown, MA 02172-0001
2	ATTN: SLCMT-TML
1	Author

U.S. Army Materials Technology Laboratory
Watertown, Massachusetts 02172-0001
FATIGUE RESISTANT OPTICAL FIBERS
George G. Bryant

Technical Report MTL TR 91-17, May 1991, 33 pp- illus-tables, D/A Project: ID464810DC26

AD_____
UNCLASSIFIED
UNLIMITED DISTRIBUTION

Key Words

Fiber optics
Dynamic tests
Fatigue tests

Certain requirements in commercial and military communications and guidance systems have prompted the development of high-strength, fatigue-resistant optical fibers for uncabled applications. The most significant environmental factors degrading the strength of glass fibers over time are stress and hydroxyl ion attack on glass surfaces. Several solutions have been formulated and attempted; these include increased bulk-strength glass and hermetic or passivating coatings. Test and evaluation of several commercially available fibers incorporating these promising solutions have been made using various fatigue and aging scenarios. Static-fatigue prediction from analysis of various constant extension rates to failure, termed in the literature and here as dynamic-fatigue, was also investigated.

U.S. Army Materials Technology Laboratory
Watertown, Massachusetts 02172-0001
FATIGUE RESISTANT OPTICAL FIBERS
George G. Bryant

Technical Report MTL TR 91-17, May 1991, 33 pp- illus-tables, D/A Project: ID464810DC26

AD_____
UNCLASSIFIED
UNLIMITED DISTRIBUTION

Key Words

Fiber optics
Dynamic tests
Fatigue tests

Certain requirements in commercial and military communications and guidance systems have prompted the development of high-strength, fatigue-resistant optical fibers for uncabled applications. The most significant environmental factors degrading the strength of glass fibers over time are stress and hydroxyl ion attack on glass surfaces. Several solutions have been formulated and attempted; these include increased bulk-strength glass and hermetic or passivating coatings. Test and evaluation of several commercially available fibers incorporating these promising solutions have been made using various fatigue and aging scenarios. Static-fatigue prediction from analysis of various constant extension rates to failure, termed in the literature and here as dynamic-fatigue, was also investigated.

U.S. Army Materials Technology Laboratory
Watertown, Massachusetts 02172-0001
FATIGUE RESISTANT OPTICAL FIBERS
George G. Bryant

Technical Report MTL TR 91-17, May 1991, 33 pp- illus-tables, D/A Project: ID464810DC26

AD_____
UNCLASSIFIED
UNLIMITED DISTRIBUTION

Key Words

Fiber optics
Dynamic tests
Fatigue tests

Certain requirements in commercial and military communications and guidance systems have prompted the development of high-strength, fatigue-resistant optical fibers for uncabled applications. The most significant environmental factors degrading the strength of glass fibers over time are stress and hydroxyl ion attack on glass surfaces. Several solutions have been formulated and attempted; these include increased bulk-strength glass and hermetic or passivating coatings. Test and evaluation of several commercially available fibers incorporating these promising solutions have been made using various fatigue and aging scenarios. Static-fatigue prediction from analysis of various constant extension rates to failure, termed in the literature and here as dynamic-fatigue, was also investigated.

U.S. Army Materials Technology Laboratory
Watertown, Massachusetts 02172-0001
FATIGUE RESISTANT OPTICAL FIBERS
George G. Bryant

Technical Report MTL TR 91-17, May 1991, 33 pp- illus-tables, D/A Project: ID464810DC26

AD_____
UNCLASSIFIED
UNLIMITED DISTRIBUTION

Key Words

Fiber optics
Dynamic tests
Fatigue tests

Certain requirements in commercial and military communications and guidance systems have prompted the development of high-strength, fatigue-resistant optical fibers for uncabled applications. The most significant environmental factors degrading the strength of glass fibers over time are stress and hydroxyl ion attack on glass surfaces. Several solutions have been formulated and attempted; these include increased bulk-strength glass and hermetic or passivating coatings. Test and evaluation of several commercially available fibers incorporating these promising solutions have been made using various fatigue and aging scenarios. Static-fatigue prediction from analysis of various constant extension rates to failure, termed in the literature and here as dynamic-fatigue, was also investigated.